ADDIS ABABA UNIVERSITY

ADDIS ABABA INSTITUTE OF TECHNOLOGY

SCHOOL OF CHEMICAL AND BIO ENGINEERING

Adsorption of Methylene Blue Dye from Synthetic Wastewater using Chitosan/graphite Composite Adsorbent; Statistical Optimization

BY

Soliyana Teshome

Advisor

Dr. Shimelis Kebede (PhD)

A Thesis Submitted to the School of Chemical and Bio Engineering as Part of the Partial Fulfillment of the Requirements for the Degree of Masters Science (Chemical and Bio Engineering in the Environmental Engineering Stream).

ADDIS ABABA UNIVERSITY

ADDIS ABABA ETHIOPIA

NOVEMBER, 2023

Approval Page

This is to certify that the thesis prepared by Ms. Soliyana Teshome entitled "**Adsorption of Methylene Blue Dye from Synthetic Wastewater using Chitosan/Graphite Composite Adsorbent; Statistical Optimization**" and submitted as partial fulfillment of the requirements for the award of the degree of master of science in chemical engineering (environmental engineering stream) complies with the regulations of the university and meets the accepted standards concerning content, quality, and originality.

Approved By the Examining Board:

Chairman, School's Graduate Committee	_____ Signature	_____ Date
Dr. Shimelis Kebede Advisor	_____ Signature	_____ Date
_____ External Examiner	_____ Signature	_____ Date
_____ Internal Examiner	_____ Signature	_____ Date

Declaration

I hereby declare that this research entitled "**Adsorption of Methylene Blue Dye from Synthetic Wastewater Using Chitosan/Graphite Composite Adsorbent; Statistical Optimization"** is based on my original work, toward the MSc degree and that, to the best of my knowledge, it contains no material previously published by another person nor material which has been accepted for the award of any other degree of the University, except where due acknowledgment has been made in text.

Soliyana Teshome ……. …….

Signature date

Abstract

The study aimed to synthesize a chitosan/graphite composite (CGC) for methylene blue dye removal from synthetic wastewater using the impregnation method. Expanded graphite was prepared by reacting graphite with H_2SO_4 and H_2O_2 at room temperature, then washed, dried, and heated. The specific surface area of graphite increased from 1193.75m2/g to 1223.648m2/g. The composite adsorbent material was synthesized using the impregnation method, with chitosan to expanded graphite ratio of 75:25. The CGC was characterized using Fourier transform infrared spectroscopy, X-ray diffraction, Brunauer-Emmett-Teller (BET) method, scanning electron microscope (SEM), and point of zero charge analysis. The optimized experimental design resulted in 98.61% removal efficiency at initial concentration of 5.24 mg/L, pH of 9.98 and contact time of 95.43. The adsorption of methylene blue dye onto CGC was best fitted with Langmuir isotherm, with an R^2 value of 0.9974 and adsorption capacity of 98g/g. The kinetics of adsorption were best fitted to pseudo-second order with an R^2=99.39.

Keywords: Adsorption, Chitosan/graphite composite, Methylene blue dye, Optimization

Acknowledgment

First and foremost, I would like to thank the almighty God who gave me the health and strength to accomplish this research work. I would like to express my gratitude to my advisor Dr. Shimelis Kebede for his valuable guidance, encouragement, and motivation throughout this study. Moreover, I would like to thank the Addis Ababa Institute of Technology, School of Chemical and Bioengineering laboratory assistants for their technical support. And finally, I am grateful to thank my family and friends for their continuous encouragement and endless support.

Contents

Approval Page i

Declaration ii

Abstract iii

Acknowledgment iv

List of Abbreviations and Acronyms ix

List of Tables x

List of Figures xii

1. Introduction 1

1.1. Background of the Study 1

1.2. Statement of the Problem 3

1.3. Objectives 4

1.3.1. General Objective 4

1.3.2. Specific Objectives 4

1.4. Significance of the Study 4

1.5. Scope of the Study 4

2. Literature Review 6

2.1. Water Pollution 6

2.2. Dyes 6

2.2.1. Sources of Dyes 6

2.2.2. Classification of Dyes 7

2.3. Methylene Blue Dye 7

2.3.1. Health Impacts of Methylene Blue Dye 7

2.3.2. Applications of Methylene Blue Dye 8

2.4. Methods of Dye Removal from Wastewater 8

2.5. Adsorption 9

2.5.1. Physical Adsorption 10

2.5.2. Chemical Adsorption 10

2.6. Factors Affecting Adsorption Process 10
2.6.1. Initial Dye Concentration 10
2.6.2. pH 11
2.6.3. Effect of Contact Time 11
2.7. Chitosan 12
2.7.1. Applications of Chitosan 12
2.7.2. Extraction and Uses of Chitosan as Adsorbent 12
2.8. Expanded Graphite 13
2.9. Summary of Previous Studies on the Removal of Methylene Blue Dye 13
3. Materials and Methods 15
3.1. Chemicals and Equipment 15
3.1.2. Apparatus and Equipment 15
3.2. Raw Material Treatment and Sample Preparation 16
3.2.1. Raw Material Collection 16
3.3. Preparation of Expanded Graphite 16
3.4. Synthesis of Chitosan/graphite Composite 16
3.5. Mixing Ratio Determination 17
3.6. Particle Size Determination 18
3.7. Physicochemical Characterization of Chitosan/graphite Composite Adsorbent Material 18
3.7.1. Point of Zero Charge Analysis 18
3.7.2. Specific Surface Area Characterization 19
3.7.3. X-Ray Diffraction (XRD) Analysis 19
3.7.4. Fourier Transform Infrared Spectroscopy (FTIR) Analysis 20
3.7.5. Scanning Electron Microscope (SEM) Analysis 20
3.8. Preparation of Adsorbate Solution 21
3.9. Individual Effect of Parameters on the Adsorption Process 22
3.10. Study of Interaction Effect of Process Parameters and Model Evaluation Using Box-Behnken Design Response Method 23
3.10.1. Independent Factors and Their Codded Levels for BBD Experiments 24
3.10.2. Experimental Setup 25

3.11. Optimization of Process Parameters and Statistical Analysis 25
3.12. Adsorption Isotherms and Kinetic Studies 26
3.12.1. Adsorption Isotherms 26
3.12.2. Kinetic Studies 27
4. Result and Discussion 30
4.1. Effect of Mixing Ratio on Removal Efficiency 30
4.2. Physicochemical Characterization of Graphite, Expanded graphite, and Chitosan/graphite composite adsorbent 30
4.2.1. Specific Surface Area Analysis 30
4.2.2. X-Ray Diffraction (XRD) Analysis 31
4.2.3. Fourier Transform Infrared Spectroscopy (FTIR) Analysis 32
4.2.4. Scanning Electron Microscope (SEM) Analysis 33
4.2.5. Point of Zero Charge 34
4.3. Adsorption Experiment and Effect of Individual Parameters 35
4.3.1. Effect of Particle Size 35
4.3.2. Effect of pH of Solution 35
4.3.3. Effect Adsorbent Dosage 37
4.3.4. Effect of Initial Concentration of Methylene Blue Dye 38
4.3.5. Effect of Contact Time 39
4.4. Statistical Analysis and Adsorption Performance 40
4.4.1. Sequential Model Sum of Squares 40
4.4.2. Analysis of variance (ANOVA) 41
4.4.3. Combined Effect of Process Parameters 45
4.4.4. Statistical Optimization of Process Variables 47
4.5. Adsorption Isotherm and Kinetic Studies 49
4.5.1. Adsorption Isotherms 49
4.6. Study of Adsorption Kinetics 51
5. Conclusion and Recommendation 53

5.1. Conclusion 53
5.2. Recommendation 54
References 55
Appendix 66
Appendix A: The Effect of Chitosan/graphite Mixing Ratio, and Particle Size on the Removal 66
Appendix B:-Point of Zero Charge Analysis for Chitosan/Graphite Composite 66
Appendix C: Individual Effect of Operating Parameters on Removal of Methylene Blue Dye 67
Appendix D: Adsorption Isotherm and Kinetic Model Data 68
Appendix E: Data from Design Expert Model Fitting 68

List of Abbreviations and Acronyms

Abbreviation and Acronym	Meaning
ABS	Absorbance
AC	Activated Carbon
ANOVA	Analysis of Variance
BBD	Box-Behnken Design
BET	Brunauer, Emmett, and Teller
CGC	Chitosan/graphite Composite
Cs	Chitosan
CV	Coefficient of Variation
FTIR	Fourier-Transform Infrared Spectroscopy
GLA	Glutaraldehyde
HCl	Hydrochloric Acid
MB	Methylene Blue
RSM	Response Surface Methodology
SEM	Scanning Electron Microscope
USEPA	United States Environmental Protection Agency
XRD	X-ray Diffraction

List of Tables

Table 2. 1: Advantages and disadvantages of some dye removal methods from waste water 9

Table 3.1: Absorbance value of methylene blue dye concentration at 663 nm 21
Table 3.2: Factors and their study level for the OVAT preliminary experiment 23
Table 3.3: Independent factors and their coded level for the BBD experiment 24
Table 3.4: BBD design matrix for three factors 25

TABLE 4.1: BET texture properties of graphite, expanded graphite, and chitosan/graphite composite 31
Table 4.2: Sequential model sum of squares 41
Table 4.3: Analysis of variance (ANOVA) table 42
Table 4.4: Fit statics 43
Table 4.5: Working condition of factor and response for optimization 48
Table 4.6: The model predicted and observed response of optimization 48
Table 4.7: Parameters of isotherm for MB dye adsorption onto chitosan/graphite composite 50
Table 4.8: Kinetic model parameters for adsorption of MB dye onto chitosan/graphite composite 51

Table A-1: Effect of chitosan/graphite mixing ratio on the removal of methylene blue dye using chitosan/graphite composite synthesized with (1:3, 1:1 and 3:1) ratios 66
Table A-2: Effect of particle size on the removal of methylene blue dye using chitosan/graphite composite 66

Table B-1: Point of zero charge for chitosan/graphite composite 66

Table C-1: Effect of pH of the solution on the removal of methylene blue dye using chitosan/graphite composite 67
Table C-2: Effect of initial concentration of methylene blue dye 67
Table C-3: Effect of contact time 67

Table D-1: Equilibrium data for adsorption isotherm model 68

Table D-2: Equilibrium data for adsorption kinetics models..... 68

Table E-1: Model summary of statistics for methylene blue dye removal..... 68
Table E-2: Fit statics for methylene blue dye removal..... 69

List of Figures

Figure 2. 1: Chemical structure of methylene blue dye (Tichapondwa et al., 2020) 7

Figure 2.2: Chemical structure of chitosan (Saheed et al., 2021). 12

Figure 3.1: Process flow diagram of research experimental work..... 16

Figure 3.2: Preparation of chitosan/graphite composite 17

Figure 3.3: Calibration curve for methylene blue dye 22

Figure 4.1: Effect of mixing ratio on the removal of methylene blue dye..... 30
Figure 4.2: XRD diffraction of graphite, expanded graphite, and chitosan/graphite composite 32
Figure 4.3: FTIR Spectra of graphite, expanded graphite, and chitosan/graphite composite 33
Figure 4.4: SEM image of a). Graphite, b). Expanded graphite and c). Chitosan/graphite Composite.... 34
Figure 4.5: Point of zero charge of chitosan/graphite composite 34

Figure 4.6: Effect of particle size on adsorption of methylene blue dye 35
Figure 4.7: Effect of pH on adsorption of methylene blue dye..... 37
Figure 4.8: Effect of adsorbent dosage on adsorption of methylene blue dye..... 38
Figure 4.9: Effect of initial concentration on adsorption of methylene blue dye 39
Figure 4.10: Effect of contact time on adsorption of methylene blue dye..... 40
Figure 4.11: Normal plot of residual for removal efficiency..... 44
Figure 4.12: Residual versus run for removal efficiency..... 44
Figure 4.13: Predicted VS Actual Plot for Removal Efficiency 45
Figure 4.14: Interaction effect of a).pH VS initial concentration, b).Contact time VS initial concentration, C). Contact time VS pH..... 47
Figure 4.15: Langmuir (A) Freundlich (B) models for methylene blue dye adsorption using chitosan/graphite composite..... 50
Figure 4.16: Pseudo-first order (A) and pseudo-second-order (B) 52
Figure -4. 17: Some experimental photos..... 69

1. Introduction

1.1. Background of the Study

One of the main global concern is water pollution. The ecology is getting worse due to the industrialization and urbanization. Water pollution has become as world's environmental concern because it is necessary for life. About 2 million tons of different types of waste are discharged into water bodies worldwide (Vasilachi et al., 2021). Various industries such as leather, textile plastic, refineries, printing petroleum, and pharmaceutical industries contribute to the contamination of water bodies by discharging organic and inorganic pollutants (Eltaweil et al., 2020). This water pollution is caused due to the discharge of various toxic chemical compounds such as heavy metals, pesticides, insecticides, hydrocarbons, and pharmaceutical products (Elwakeel et al., 2021). From this perspective, scientists were motivated to get those hazardous elements get removed out of the waste water. The most significant courses of water contamination are determined to be dyes. Dyes can have negative health and environmental consequences such as turbidity eutrophication, bioaccumulation, and mutagenicity (Elwakeel et al., 2021). In addition to this, they can have a long term negative impact on the aquatic life by disturbing their photosynthesis and germination activities (Solayman et al., 2023).

Methylene blue dye is among the most commonly used dye staffs in dying cotton, silk, leather, paper, and hair industries (Song et al., 2022). The dose and length of exposure to methylene blue dye can lead to various health problems. Taking methylene blue dye by mouth can cause a burning sensation, vomiting, sweating, mental confusion, and nausea. Exposure to a large amount of methylene blue dye cause bad headache and chest and abdominal pain (Al-Graiti & Merdas, 2023). The rapid industrial development along with the consumption of dye increases the amount of dye discharged into the surrounding receiving water bodies (Arunachalam, 2021). More than 100,000 types of dyes exist commercially. It is believed that more than 700,000 tons of dye are produced annually with 10 to 15% of this amount discharged to water bodies. The discharge of produced effluent into the aquatic environment causes serious health problems and affects aquatic life by decreasing the light penetration capacity of water which disturbs their photosynthesis activity (Pathirana et al., 2023). Therefore, there is a need for a cost-effective, easy, and efficient removal mechanism to the permissible level before discharge into the surroundings.

Various treatment mechanisms such as chemical coagulation, biological degradation, and oxidation and adsorption methods have been employed. However, the biological and chemical methylene blue dye removal mechanisms are complex and costly (Myneni et al., 2020). Among those MB removal methods, the adsorption method gained great attention. This is due to the advantages of simple operational procedures, high efficiency, low cost, and capacity to produce secondary pollutants which can result from oxidation degradation of methylene blue dye and reusability (Santoso et al., 2020).

Chitosan is a naturally abundant material. It contains multi fascinating functional group like amino, carboxyl and hydroxyl groups. Moreover, chitosan contains important physicochemical properties like high reactivity and high selectivity towards pollutants. However, some drawbacks such as poor stability, law mechanical strength, and solubility pattern (solubility below pH 5) limits the use of crude chitosan as an adsorbent (Moosa et al., 2016). In the recent years, physical and chemical modification of chitosan have attracted the attention of researchers to obtain improved physical and chemical properties of chitosan beads (Quach & Doan, 2023). Graphite is the most stable allotrope carbon. The special sandwich stricture along with the distance between the interlayers make it suitable to incorporate materials between the layers. The distance between the interlayer and porosity can be increased by heating intercalating substance on graphite (Kyzas et al., 2015).

The benefits of an efficiency of adsorption mechanism is determined by the type and qualities of adsorbent material utilized. Because of its availability, ease of modification, and good pollutant selectivity, chitosan/expanded graphite was used in this research investigation to remove methylene blue dye from synthetic waste water (Doondani et al., 2022).

1.2. Statement of the Problem

Dye molecules, as large group of molecules, have Couse much public health concern. Methylene blue dye is one the most comely used and discharged dye staff from paper and pulp, chemical, textile, and dye manufacturing industries. The existence of MB dye beyond the recommended limit courses a functional disorder on the kidney, reproductive system, liver, brain, and central nervous system (Gemici et al., 2021). It affects aquatic life by disturbing their photosynthesis activity by decreasing the light penetration capacity of water (Oyewo et al., 2020). Conventional treatment methods, such as coagulation-flocculation, ion exchange, reverse osmosis, advanced oxidation, and membrane filtration have been employed for the removal of methylene blue dye from water and waste water (Barus et al., 2022). However, those treatment methods have several limitations such as high operational and maintenance costs, high energy requirements, and production of secondary pollutants (Murcia-Salvador et al., 2019).

Among those treatment methods, adsorption has become an efficient technique due to its ease of operation, low operational cost, simplicity of design, high removal efficiency, and the existence of various adsorbent alternatives (Amar et al., 2020). The most important point on adsorption is the type of adsorbent material used. In the recent years, the need for preparation of efficient, eco-friendly, involving simple operational procedures, biodegradable, biocompatible, green and improved physicochemical properties adsorbent material has become as essential research interest (VO, 2021). Chitosan is the most important material derived from chitin, the second most abundant material next to cellulose. (Chouhan & Mandal, 2021). Even though chitosan has amino ($^{-}NH_2$) and hydroxyl (OH^{-}) important functional groups for adsorption applications, it needs a modification to improve its physic chemical properties (Kahya & Erim, 2021).

Researchers has been try to modify chitosan to improve its physico-chemical properties. Different substances such as, graphene, graphene oxide, and magnetite and graphene oxide have used to form composite with chitosan. However most of the modification process involves multi step procedure, with consumption of many chemicals. Moreover, researchers did not focus on the optimization of process parameters that affect the adsorption process. So; modification of chitosan that involves simple fabrication to obtain novel adsorbent material and optimization of process parameters is needed.

1.3. Objectives

1.3.1. General Objective

The general objective of this study is to prepare a chitosan/graphite composite adsorbent for the efficient removal of methylene blue dye.

1.3.2. Specific Objectives

The Specific Objective of This Research is to;

- Prepare chitosan/graphite composite adsorbent using the impregnation method;
- Characterize the physicochemical properties of chitosan/graphite composite adsorbent (using point of zero charge, XRD, SEM, BET, and FTIR);
- Study the individual and interaction effect of variables (chitosan/graphite mixing ratio, pH of the solution, adsorbent dosage, initial dye concentration, particle size, and contact time)
- Statistically optimize the removal efficiency of composite adsorbent using RSM;
- Investigate the kinetics and adsorption capacity of chitosan/graphite composite on the removal of methylene blue dye from synthetic wastewater;

1.4. Significance of the Study

The discharge of colored effluent into the environment results in serious environmental problems. Therefore, the successful completion of this paper is significant to various stakeholders including dye manufacturing industries and textile industries. The use of composite adsorbent can offer useful information about the optimum composition and operating parameters for the efficient removal of dye in colored wastewater treatment. The use of composite adsorbent is advantageous compared to the others in the efficiency of operation with minimum cost and sludge formation.

1.5. Scope of the Study

To achieve the above-mentioned overall goals, the scope of the study should be addressed in the following manner. The adsorbent was prepared from chitosan which is the derivative of the second most material chitin and graphite in a two-step process that includes thermal expansion of graphite and synthesis of chitosan/graphite composite by the impregnation method using different mixing proportions. The characterization covers surface functional groups using FTIR, surface morphology using SEM, specific surface area using surface area analyzer, and the crystal and

amorphous structure of both expanded graphite and chitosan/graphite were analyzed using XRD. The absorptive capacity of the prepared chitosan/graphite composite on the removal of methylene blue dye was conducted in a batch-wise process. A preliminary experiment was conducted to see the individual effect process parameters. The interaction effect parameters (contact time, and initial concentration of methylene blue dye, initial solution PH) followed by statistical optimization of removal efficiency using the RSM (BBD) method was determined. The adsorption isotherm and kinetic rate were investigated.

2. Literature Review

2.1. Water Pollution

Access to safe and reliable potable water has become a major concern of the global community, especially in undeveloped and developing countries. About 800 million people face a lack of potable water in the world. Only 39% of the sub-Saharan African population and 46% of Oceania people have access to potable water (Yunusa et al., 2021). Internationally, the amount of water contamination is increasing at an alarming rate. This rapid contamination resulted from the discharge of heavy metals, dyes, and organic and inorganic pollutants from paper, textile, printing, and leather industries in the ground and surface water (R. Ahmad & Ansari, 2021). Among those contaminants, the contribution of dyes is becoming a major public concern. This is the result of a wide range of applications which creates a high possibility to enter into the environment. The aromatic structure of most synthetic dyes gives a xenobiotic and non-biodegradable nature. As a result efficiency removal mechanism for those pollutants should be developed (Gautam & Hooda, 2020).

2.2. Dyes

The rapid population growth, unplanned urbanization, and modern industrialization results in the discharge of huge amount of contaminants in most parts of the globe (Adel et al., 2021). Especially as an important part of life, water pollution concerns everyone. The existence of dye threatens the ecosystem and can endanger human health. Anthropogenic activities are the main contributor to environmental pollution (Abdelfatah et al., 2021).

2.2.1. Sources of Dyes

The rapid growth of modern industry releases huge amounts of dye-contaminated wastewater into the environment, including water bodies. Dye-loaded wastewater mainly emerges from anthropogenic activities such as paper, plastic food, cosmetics, and, textile industries The existence of even a low concentration of dyes is highly visible which affects the aquatic life by decreasing the light penetration capacity of water (Liu, 2020).

2.2.2. Classification of Dyes

The color and properties of dye are determined by the chemical stature of dye molecules. Dyes can be categorized as cationic and anionic depending on their chemical structure. Dyes like that of the MB, malachite green (MG), rhodamine B (Rh), crystal violet, rhodamine 6G, and safranin O (SO) with a cationic functional group (which produces a positive charge in aqueous solution are categorized as cationic dyes. Anionic dye possesses reactive, direct, and acid dyes such as MO, acid orange7 (AO7), acid red 14 (AR14) and (Farooq et al., 2022). They can also classified as natural and synthesize their source from where they are extracted. Natural dyes are those extracted from animals, plants, and minerals. The naturally extracted from jackfruit, onion, eucalyptus, turmeric, weld, and henna had wide applications in textile industries. However rapid industrialization and an increase in demand for dye raise interest to search for an alternative satisfactory dye product (Ngulube et al., 2017).

2.3. Methylene Blue Dye

Methylene blue dye ($C_{16}H_{18}ClN_3S.XH_2O$) is a sapphire cationic dye that belongs to the phenothiazine family. It is one of the most commonly used dye staff. MB is used as a colorant, biological stain, and redox indicator. Industries such as leather, cotton, paper, and silk industries use MB extensively as colorants. In most industries, it is discharged with a concentration of 10-20mg/L into the receiving water bodies (Radoor et al., 2021). Compared to other dye staff methylene blue dye is stable and highly resistance to oxidation and photolysis (Han et al., 2021).

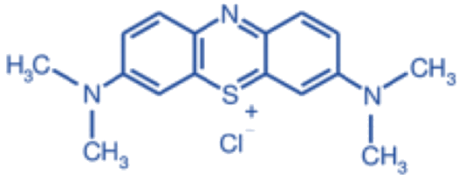

Figure 2. 1: Chemical structure of methylene blue dye (Tichapondwa et al., 2020)

2.3.1. Health Impacts of Methylene Blue Dye

Despite its wide range of applications, it causes various negative impacts on human health and the aquatic ecosystem. Exposure to such types of effluent can cause serious health problems including

increasing heart rate, vomiting, difficulty to breath, vomiting, and burning of the eye, mouth, and throat (Miraboutalebi et al., 2017).

2.3.2. Applications of Methylene Blue Dye

Methylene blue dye is mainly used in the industrial sectors for coloring paper, cotton, and silk dying processes. It is also widely used in the medical sector as a treatment for Alzheimer's pain reducing the amylose burden in the patient's brain, and treatment for falciparum malaria in children and as an antidepressant. In addition to this, it also plays a great role in microscopic discoveries by using methylene blue dye as a staining agent including the identification of mycobacterium tuberculosis (Schirmer et al., 2011).

2.4. Methods of Dye Removal from Wastewater

The permissible concentration limit for methylene blue dye set by the Environmental Protection Agency is 0.2 mg/L (Thabede et al., 2020). The existence of methylene blue dye over the permissible limit causes a serious problem for human health and the environment. Various methods have been developed for the removal of methylene blue dye from industrial wastewater. The removal techniques include 1. Chemical (coagulation-flocculation, photolytic degradation, and, an electrochemical treatment (Kuang et al., 2020). 2. Biological and 3. physical (Membrane filtration, ion exchange, and adsorption (Jaiswal et al., 2021). The chemical treatment method is an efficient waste water treatment method. However, its application is limited by the production of secondary pollutants, high cost, and high consumption of electrical energy (Malatji et al., 2021). The biological treatment involves the conversion of dye molecules into simple and harmless compounds by using biological organisms such as plants, algae, fungi, and bacteria. The degradation process can be undergone under aerobic or anaerobic processes. Compared to the other methods the biological treatment is eco-friendly. Moreover has minimum chemical and energy consumption (Musa & Idrus, 2021). However, the requirement of a certain amount of land for bioreactor, complex operational procedure, and strict environmental conditions limits the use of biological treatment. In addition to this, the complex chemical structure of dye molecules has made the resistant to biological degradation (Zhou et al., 2019). Physical treatment methods such as membrane filtration, ion exchange, and adsorption have also effective removal of methylene blue dye. However, the application of membrane filtration is difficult in the disposal of solids left

after filtration and the inability to remove the dissolved component of the given pollutant (Agboola et al., 2021).

Among the developed waste water treatment technologies the adsorption treatment method attracts the attention of many researchers. The adsorption method is found a promising treatment mechanism for the removal of methylene blue dye. The removal efficiency of the adsorption mainly depends on the properties of the adsorbent material such as specific surface area, cost, eco-friendliness porosity, selectivity, reusability, and crystal structure (Rashid et al., 2021). The adsorption treatment method has become a wide treatment mechanism due to its high efficiency, law operation and maintenance cost, simplicity of design, low initial cost existence of a wide range of adsorbent materials (Tran et al., 2021).

Table 2. 1: Advantages and disadvantages of some dye removal methods from waste water

Physical /chemical method	Advantages	Disadvantages
Photochemical oxidation	Rapid process Good sorption capacity for dye	Formation of byproduct High energy cost
Electrochemical	Effective for basic dyes	High cost of electricity
Activated carbon	Remove all dyes No adsorbent loss	Very expensive
Silica	Effective depolarization	Side reaction in effluent Concentrated sludge production
Membrane technology	Environmentally friendly	Not effective for dye removal
Ion exchange	Low cost Good general ability	Les efficient for a column of flow adsorption system

2.5. Adsorption

Adsorption involves the movement of adsorbate (solute) from a gas or liquid solution to the adsorbent (solid surface) through a chemical or physical bond. Adsorption techniques can be applied for both organic and inorganic pollutants in both water and wastewater treatment methods. The adsorption process can be affected by several factors. The adsorption of methylene blue dye is influenced by contact time, the initial pH of the effluent, the dosage of adsorbent, and the initial

concentration of dye. The attention of many researchers has been drawn to adsorption methods in recent years. The adsorption method has been determined to be the most efficient treatment mechanism. The united States environmental protection agency reports the adsorption has a low operating cost, higher removal efficiency, rapid reaction rate, and simple design and operation (S. Singh et al., 2023). Various chitosan-based adsorbent materials have been employed for the removal of methylene blue dye from water and wastewater including chitin, grafted chitosan,

2.5.1. Physical Adsorption

Physical adsorption occurs when the adsorbent and adsorbate are held together with weak forces. During the physical adsorption process, the adsorbent and adsorbate molecules are held by the weak van der Waals, force, dipole-dipole force of hydrogen bonding. Moreover, the physical adsorption process is reversible and non-selective and undergoes small enthalpy changes usually 40-125kJ/mol (Mashkoor & Nasar, 2020).

2.5.2. Chemical Adsorption

Chemical adsorption is adsorption where the adsorbent and adsorbate are held by a strong chemical bond, usually an ionic or covalent bond. This strong interaction makes chemical adsorption irreversible. Unlike physical adsorption in chemical adsorption, the adsorbate forms a mono-molecular layer on the surface of the adsorbent. Chemical adsorption takes place under higher enthalpy change usually 30-400kJ/mol (Fakher & Imqam, 2020).

2.6. Factors Affecting Adsorption Process

2.6.1. Initial Dye Concentration

The amount of dye removed is highly influenced by the initial concentration of dye in the solution. The removal efficiency is influenced by the relationship between the initial concentration of the adsorbate and the active site on the surface of the adsorbent. The effect of the initial concentration of methylene blue on the removal efficiency of chitosan/graphite composite is mainly related to the ratio amount of dye molecules present in the give solution and the available active site of adsorbent surface for adsorption. Generally, an increase in dye concentration results in decreases in the percentage of removal. Because as the concentration of dye increases, there will be a lack

of active site into which adsorbate material will bind (N. Singh et al., 2019). Research conducted by (Nayl et al., 2022) reports that the removal efficiency decreases with an increase in the initial concentration of methylene blue dye. The initial concentration increased from 10-50 mg/L, resulting in a sharp decrease in the percentage of removal from 99.99 to 39.3%.

2.6.2. pH

The initial pH of the solution is one the most important parameters that affect the removal efficiency of the adsorbent material. The initial pH of the solution affects the removal by changing the charges of the adsorbent surface, the electrical charge of the dye, and the degree of ionization (El-Habacha et al., 2023). The surface of the adsorbent maintains opposite charges above and below the point of zero charge. The surface of the adsorbent becomes positive below the point of zero charge and negatively charged above the point of the charge. The adsorption capacity of the adsorbent surface and the type of surface active center are related by an important factor called the point of the charge. The point of zero charge was also studied based on pH. Research conducted by (Gautam & Hooda, 2020) reported the effect of pH 2-14 on the removal efficiency of methylene blue dye by magnetic grapheme oxide/ chitin Nano-composite for 20mg adsorbent of 5ml dye solution at 298k. The best removal efficiency was observed at a pH of 10 reaching 61.3mg/L% of removal.

2.6.3. Effect of Contact Time

The contact time between the adsorbent and the adsorbate plays a great role in the adsorption process. The rapid uptake and shorter equilibrium time imply the efficiency of the adsorbent material (Ethaib & Zubaidi, 2020). As reviewed in many literature the rate of adsorption is rapid at the initial stage. The rapid uptake in the initial stage is the result of the availability of free vacant space on the adsorbent material for adsorption. However, the rate of adsorption becomes slow near equilibrium. The reason for the slowest uptake near equilibrium is due to the absence of a free active site for further adsorption process. The study reported by (Yan et al., 2019) the study of the effect of contact time on the removal of methylene blue dye by chitosan cross-linked graphene oxide /lignosulfonate composite aerogel from (0-300) minutes to remove 50mg/L, 80mg/L, and 100mg/L initial concentration with 0.05 adsorbent dosage. The result shows a rapid uptake for the first 40 minutes and increases slightly up to 300 minutes.

2.7. Chitosan

Chitosan is a chitin derivative which is obtained by partial de-acetylation of chitin. Chitin is the second most abundant biopolymer next to cellulose on the earth. It is usually derived from natural sources such as residues of shrimp, crab, lobster, fungal mycelia, and green algae. Chitin is a material that is discarded in fish processing industries. The extraction of chitosan from chitin and its use as alternative adsorbent material can reduce waste in the environment (Murcia-Salvador et al., 2019). Chitosan has an amino, primary, and secondary hydroxyl group. Chitosan's high affinity for various organic and inorganic pollutants is due to the presence of functional groups that act as active sites. Chitosan's high affinity for various organic and inorganic pollutants is due to the presence of functional groups that act as active site.Properties such as high porosity, biocompatibility, biodegradability, and producing different toxic byproducts make chitosan gain high attention to be used as an adsorbent in various industries (Zango et al., 2022).

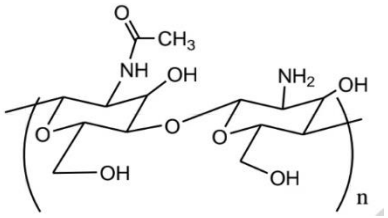

Figure 2.2: Chemical structure of chitosan *(Saheed et al., 2021).*

2.7.1. Applications of Chitosan

Chitosan has various commercial applications in waste water treatment, food preservation, cosmetics as dehydrating agents, and hydrogel film in pharmaceutical areas (Ke et al., 2021).

2.7.2. Extraction and Uses of Chitosan as Adsorbent

Chitosan can be extracted from chitin using the chemical method or enzymatic method of treatment. A chitin with more than 50% degree of deacetylation is called chitosan. The chemical method involves demineralization, and depolarization followed by deacetylation with the help of NaOH. However, the chemical treatment method has high energy consumption and generation of secondary pollutants (Wang et al., 2020). Problems associated with the production of secondary pollutants can be overcome by enzymatic method. The demineralization process (removal of

CaCO3 with the help of NaCl) is the same for both chemical and biological methods. However, deproteinization and deacetylation methods are replaced by enzymatic reactions. The enzymatic method has also many limitations such as the high production cost of enzymes and the requirement for different types of enzymes (Kou et al., 2021).

2.8. Expanded Graphite

Expanded graphite is a carbon material that possesses important qualities of adsorbent material like that of weak polarity, hydrophilic and lipophilic nature and, high selection sorption capacity (Ji & Wang, 2012). The expansion of graphite can be carried out through thermal, chemical, and electrochemical processes. Each expansion method has its advantages and limitations. The thermal expansion of graphite is achieved through the release of gas at high temperatures between the layers. However, the non-homogenous distribution of gases results in the formation of multilayer structure. The expansion process can be also achieved through the electrochemical expansion method which is a highly efficient and eco-friendly process. Despite this, its use is limited by the production of radicals during the hydrolysis process. Relatively the chemical expansion process is superior where expansion results from the gas evaluation from a chemical reaction. However, its use is limited by the release of pollutant chemicals into the receiving environment (Ardestani et al., 2022).

2.9. Summary of Previous Studies on the Removal of Methylene Blue Dye

Various research studies have been conducted on the adsorption of methylene blue dye from wastewater using different adsorbents and operating the adsorption process on different operating parameters. (Dbik et al., 2022) used agricultural solid waste to remove methylene blue dye from an aqueous solution. They study the effect of adsorbent dosage (0.4-2.4g/L), contact time (0-120min), and initial concentration of methylene blue dye (100-500mg/L). They report the optimized result by BBD-RMS was found to be 89.48% at an adsorbent dosage of 1.78g/L, contact tome of 56 min, and initial concentration of MB 176mg/L at pH of 5.4 and $21^{O}C$. The experimental value was in close agreement with the predicted value of 0.97 R^2 value. (Belachew & Hinsene, 2022) also used zeolite 4A to remove MB from the aqueous solution. They study the adsorption process by the pH (2-10), contact time (30-180) min, adsorbent dosage (20-60) mg/L, and initial concentration of methylene blue dye (10-20) mg/L. The maximum removal efficiency which is

99.37% was found at 50ml of 10 mg/L initial concentration of MB, 39.05 mg zeolite 4A adsorbent dosage, and 179.82 min contact time. It had R^2 value=0.997 and p-value <0.0001. The individual effect of pH was optimum at pH 9 with a 6.68 point of zero charge value. Pseudo-second-order kinetics and Langmuir isotherm were best fitted. The maximum removal efficiency (Q_{max}) of zeolite 4A was 44.34mg/g. Another study on the adsorption of MB was conducted by (Mathivanan et al., 2021) using ipomoea by varying the independent; initial concentration of MB (10-50)mg/L, adsorbent dosage (0-5)g/L,and pH (2-10). The optimum removal efficiency (83.87) was at optimum conditions of initial concentration of MB 30.48 mg/L, an adsorbent dosage of 3.1g/L, pH 7.04, and a contact time of 125 min. The Langmuir isotherm model and pseudo-first-order kinetic models were best fitted. The adsorption amount was 7.53mg/g. In addition to this, the adsorption of methylene blue dye by zero-valente iron nanoparticles was synthesized from sweet lime pulp. The adsorption experiment was conducted by varying the pH (4-10), contact time (0-300) min adsorbent dosage (0.4-1.2)g/L, initial concentration of methylene blue dye (5-40) mg/L and temperature (25-45) ^{O}C. At the optimal conditions of 10mg/L initial concentration, 1.2 g/Adsorbent dosages, and 25OC temperature, the maximum removal efficiency was reported at 98.9% The Freundlich adsorption isotherm was best fitted with 0.98 R^2 value.

So; from the reported literature, it is observed that the main factors that affect the adsorption process are; the initial pH of the solution, the adsorption time, the adsorbent dosage, and the initial concentration of methylene blue dye. And the Freundlich and Langmuir isotherms were used the adsorption isotherm.

3. Materials and Methods

3.1. Chemicals and Equipment

3.1.1. Chemicals and Reagents

All chemicals used for this study were analytical grade and they were used without further purification as received. Concentrated Sulfuric acid (98%) and hydrogen per oxide (30%) were used for the preparation of expandable graphite. Acetic acid (2%) and glutaraldehyde (2%) were used to dissolve and crosslink chitosan during the preparation of the chitosan/graphite composite respectively. Chitosan from shrimp shells 75% (deacetylated) and graphite were used to prepare chitosan/graphite composite adsorbent using the impregnation method. Both sodium hydroxide (99.9% purity) and hydro chloric acid (35%) were used to adjust the pH of the solution during the investigation of the effect of the pH of the solution. Methylene blue dye ($C_{16}H_{18}ClN_3SXH_2O$) was used to prepare different working methylene blue dye concentrations. Distilled water was also used for dye solution preparation.

3.1.2. Apparatus and Equipment

The following apparatus and equipment's were used in this study. Magnetic stirrer was used to mix the solution throughout the adsorption process. UV-visible spectrophotometer (SPECTRO UV-VIS DOUBLE BEEM 8 SCANNING AUTO CELL UVD-3200) was used to measure absorbance and methylene blue dye concentration. A 45µm siring filter was used to filter chitosan/graphite composite from the mother liquor. Other instruments such as analytical balance (HS22OS), pH meter, beaker, drier, mortar, and sieve were used through the study. The surface morphology of the adsorbent was studied by scanning electron microscope (SEM). Fourier transforms infrared spectroscopy (PerkinElmer) was used to find the functional group of graphite, expanded graphite and chitosan/graphite composite. The crystal structure of graphite, expanded graphite and chitosan/graphite composite was studied by X-ray Diffraction.

3.2. Raw Material Treatment and Sample Preparation

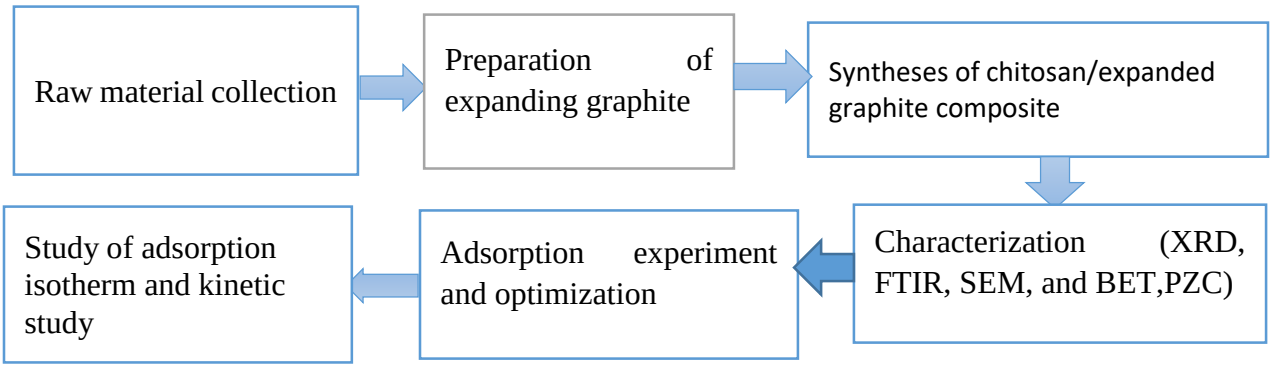

Figure 3.1: Process flow diagram of research experimental work

3.2.1. Raw Material Collection

The raw materials used for the synthesis of chitosan/expanded graphite composite adsorbent, chitosan (75% degree of deacetylated), graphite, acetic acid (2%), hydrogen peroxide (30%) and glutaraldehyde (2%) were purchased from the local suppliers in Addis Ababa, Ethiopia.

3.3. Preparation of Expanded Graphite

The method of the synthesis of expanded graphite was adopted from previous works (Ji & Wang, 2012). A known amount of graphite was weighed and added with concentrated sulfuric acid (98%), and hydrogen peroxide (30%) with (C: H_2S0_4:H_2O_2 =6g: 10ml: 1.5ml) respectively. Next, this mixture was reacted for 90 minutes by stirring with 120 rpm magnetically at room temperature to form expandable graphite. Then the mixture was washed several times with distilled water to remove residual H_2SO_4 until the pH reaches of 7. After that, the graphite was dried in a drier at a temperature of 60^{O}C for 12 hours. Finally, the expandable graphite was expanded by rapid heating at a temperature of 900^{O}C for 3 minutes in a muffle Furnace (Ji & Wang, 2012).

3.4. Synthesis of Chitosan/graphite Composite

The method for the synthesis of chitosan/graphite composite using the impregnation method was adopted from previous studies with minor modifications. A known amount of chitosan was dissolved in a known amount of acetic acid (Chitosan: Acetic acid =2g: 100ml) in three separate beakers coded as C13, C11, and C31. Then known gram of expanded graphite along with

glutaraldehyde ($C_5H_8O_2$), (Expanded graphite: glutaraldehyde=1g: 7ml) was added (Gedam et al., 2015). Chitosan to expanded graphite mixing ration in C13, C11, and C31 was 25:75. 50:50 and 75:25 respectively to choose the best mixing ratio. The mixture was stirred for 5 hours at room temperature with the help of a digital overhead stirrer with 300rpm stirring speed. After that, the mixture was washed several times and dried at a temperature of 75^{O}C for 24 hours. Finally, the adsorbent was ground and sieved with sieve**.** Note C13, C11 and C31 stands for reaction flasks holding 25:75, 50:50, and 75:25 chitosan/graphite mixing ratios.

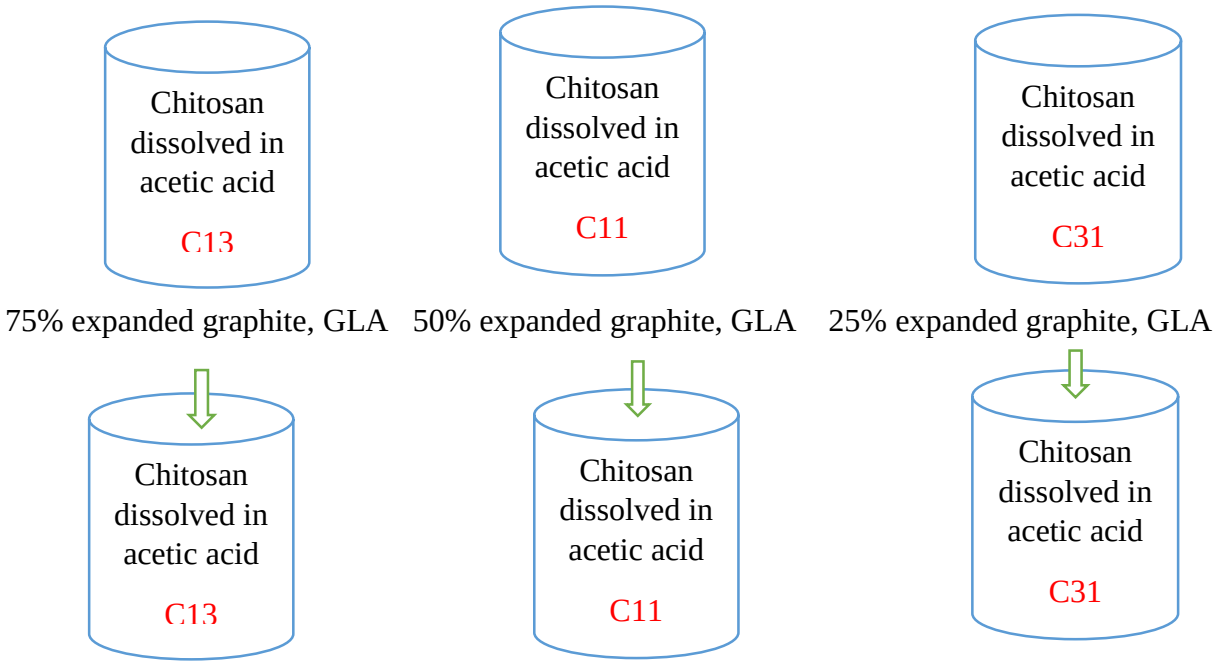

Figure 3.2: Preparation of chitosan/graphite composite

3.5. Mixing Ratio Determination

The effect of chitosan to graphite on the removal efficiency was studied by (Dongre, 2018) . An experiment was conducted by varying graphite content 5-30% to see the effect of chitosan/graphite mixing ratio. 20% chitosan doped composite was found best. However, the specific surface area of 80:20 chitosan to graphite mixing ratio was limited to 3.9 m^2/g in the range of 175-246µm particle size. In this study, the effect of the chitosan/graphite mixing ratio was determined by varying the mixing ration with 25:75, 50:50, and 75:25 at a neutral pH to remove 30mg/L concentration of a solution with 1g/L adsorbent dosage of 250-300 particle size within one hour. The optimum mixing ratio was selected for further studies.

3.6. Particle Size Determination

Then an experiment was conducted on the range of 125-150 μm, (150-250) and (250-500) μm of particle size at neutral pH keeping the mixing ratio at its optimum (i.e. 75:25) to remove 30mg/l solution with 1mg/L dosage of each size for one hour. The optimum particle size was selected for further studies.

3.7. Physicochemical Characterization of Chitosan/graphite Composite Adsorbent Material

Physicochemical characterization of graphite expanded graphite, and chitosan/graphite composite was investigated using the following technique. The surface functional group of the raw graphite expanded graphite, and chitosan/graphite composite adsorbent material were analyzed using the FTIR spectroscopy method. In addition to this, the surface morphology of raw graphite, expanded graphite, and the prepared chitosan/graphite sample were investigated by using a scanning electron microscope (SEM). The specific surface area was investigated by using Brunauer, Emmett, and Teller method (BET) based on adsorption and desorption isotherms of nitrogen gas at room temperature and pressure of 760mmHg. Furthermore, the crystal structure of the adsorbent was analyzed using X-ray diffraction. The point of zero charge for chitosan/expanded graphite composite was investigated by the salt addition method.

3.7.1. Point of Zero Charge Analysis

The initial pH of the solution is among the most influential variables on the methylene blue dye removal efficiency of chitosan/ graphite composite. The pH range on which the adsorption of methylene blue dye onto chitosan/graphite composite favored was chosen based on point of zero charge analysis and preliminary experiment of individual effect of initial solution pH, where the point of zero charges is the point at which the surface exhibits net zero charges or the point where the number of positive and negative charges becomes equal. The adsorption of anions is favored below the point of zero charge and the removal of cat ion is favored above the point of zero charge (Pashai Gatabi et al., 2016).

The point of zero charge of the chitosan/graphite composite was determined based on the salt addition method. To do this an aqueous 500 ml $NaNO_3$ (0.1M) was prepared and separated into

ten different reaction flasks with 40ml solution each. And the pH value was adjusted from 2-12 using NaOH and HNO_3. The initial pH of each flask was labeled and recorded. After that 0.2 g of chitosan/graphite adsorbent was added into each solution and shacked using a shaker at 150rpm for 24 hours. Next after 24 hours, the mixture was filtered and the final pH of each solution was measured. Finally, the pH change was plotted against the initial pH as shown below in figure 4.5 and the pointe of the zero charge was investigated where the pH change becomes zero ($\Delta pH=0$) (Bakatula et al., 2018).

3.7.2. Specific Surface Area Characterization

The specific surface area of graphite, expanded graphite and chitosan/graphite composite was estimated using the Brunauer-Emmett -Teller (BET) method based on adsorption and desorption of nitrogen gas at room temperature and pressure of 760mmHg from Bahirdar's University laboratory. To do this, first, the empty tube was measured and 0.08g of sample material was loaded into the tube and measured to determine the weight of the sample adsorbent. Then the adsorbent sample was degassed at a temperature of $300^{O}C$ for 1 hour to remove water and other volatile matter from the adsorbent sample. Next to this, the tubes were installed into the micrometric machine. The liquid nitrogen was filled into the dual flask and placed in the specific surface area analyzer. The specific surface area was determined based on the adsorption and desorption isotherm of nitrogen gas at a temperature of 77.3k and pressure of 760mmHg using the SA-9600 serious surf area analyzer machine.

3.7.3. X-Ray Diffraction (XRD) Analysis

X-ray diffraction (XRD) is a powerful non-depictive technique for characterizing crystalline materials. XRD analysis was performed to check whether graphite, expanded graphite, and graphite /chitosan composite were crystalline or amorphous. Each mineral type is defined and characterized by a unique x-ray pattern. The diffraction angle 2θ was varied from 5 ^{O}C to $65^{O}C$. the XRD data collection was aimed at informing the graphite structural change after being expanded and composed with chitosan. The diffraction was performed by (XRD-7000 X-RAY DIFFRACTOMETER, japan) using Bragg's law using the formula shown below (Kim et al., 2013).

$$n\partial = 2dsin\theta \quad (1)$$

Where n is an integer, ∂ is the wavelength of the X-ray d is the inter-planar spacing generating the diffraction, and θ is the diffraction angle.

3.7.4. Fourier Transform Infrared Spectroscopy (FTIR) Analysis

Fourier transform infrared spectroscopy is a powerful tool used to identify the type of chemical bond present in a molecule in the wavelength range of 4000-400 cm^{-1} by producing an infrared absorption spectrum that is like a molecular fingerprint. The infrared light absorbed at a specific frequency is directly related to the atom vibration of bond energy in the molecule. The functional groups of graphite expanded graphite, and chitosan/graphite composite were analyzed using the spectrum of the FTIR on 65 spectra FT-IR PerkinElmer machine. The sample was placed in front of the detector and monochromatic infrared radiation was emitted from the source. When the infrared light reaches the splitter which is a partial transmitter mirror some of the radiation is passed through and the remaining is reflected. The two beams reached the mirror where they were reflected to the splitter ant both beams were split again causing the part of the radiation to reflate from the fixed and move to re-combine and go through the sample into the detector. The other part of the radiation that was reflected by the mirror goes to the radiation source.

3.7.5. Scanning Electron Microscope (SEM) Analysis

The scanning electron microscope has been a fundamental tool to obtain information on the morphology of the surface and for having insight into the morphology of the adsorbent material scanning electron microscope (SEM) is used to investigate the morphology and shape of the surface of adsorbent material (Oguanobi et al., 2019). The surface morphology of raw graphite expanded graphite, and chitosan/graphite composite adsorbent was investigated using a scanning electron microscope (FEI, INSPCT-F50, Germany.) Machine at Adama science and Technology University. The SEM operating conditions to scan the raw graphite expanded graphite and chitosan/graphite composite were was1500× magnification 15kv power, 20μm scale, and vacuum pressure.

3.8. Preparation of Adsorbate Solution

A standard 1000 mg/l methylene blue dye stock solution was prepared by dissolving 1g methylene blue dye in 1L distilled water. All the other samples (5mg/L, 10mg/L, 15mg/L, 20mg/L, and 25mg/L) were prepared by diluting the stock solution into the required concentration. In this study adsorption of methylene blue dye with chitosan/graphite composite was conducted in 800 bikers by stirring magnetically of 100ml solution for a predetermined length of time. At the end of each batch adsorption experiment some amount of aliquots were taken from the reactor and filtered using 45μm syringe filter. Then the absorbance of filtrate of each sample was analyzed with (SPECTRO UV-VIS DOUBLE BEAM PC 8 SCANNING AUTO CELL uvd -3200) Spectrophotometer at 663 nm wavelength. The concentration of the standard solution was varied from 5-25mg/L and a standard calibration curve that passed through the origin was drawn using the concentration of the standard solutions and their corresponding absorbance. The calibration curve has a correlation of R^2 value 0.9977 which satisfies the beer-lamp law and validates the statistical validity of measurements. Then concentrations of each filtrate were determined by measuring its absorbance and inserting the absorbance into the equation of the standard curve. Finally, the percentage of methyl blue dye removal was calculated using the equation: -

$$\% \, Removal \; Efficiency = (\frac{C_i - C_f}{C_i}) \times 100 \tag{2}$$

Where C_i and C_f are the initial and final methyl blue dye concentration in (mg/L) respectively. All experiments were conducted according to the experimental layout

Table 3.1: Absorbance value of methylene blue dye concentration at 663 nm

Concentration	Absorbance
0	0
5	0.962
10	1.857
15	2.917
20	3.69

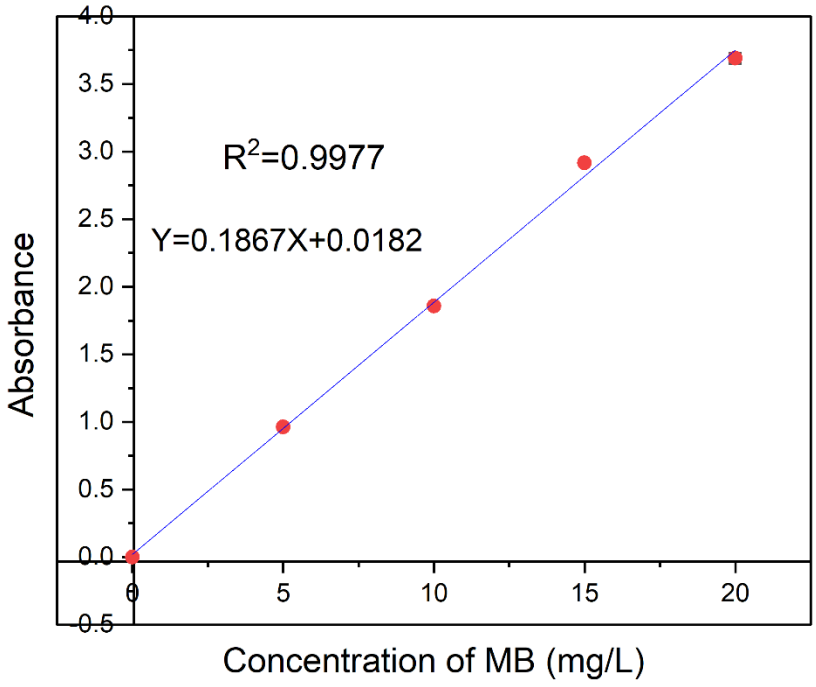

Figure 3.3: Calibration curve for methylene blue dye

3.9. Individual Effect of Parameters on the Adsorption Process

The individual effect of each variable on the methylene blue dye adsorption efficiency of the synthesis chitosan/graphite composite was studied based on one variable at a time experiment. The effect of each operating parameter was investigated with a batch adsorption experiment. Primarily a factor time experiment was conducted to investigate the individual effect of process variables (initial pH of the solution, contact time, adsorbent dosage, particle size, chitosan/graphite mixing ratio, and initial concentration of methylene blue dye) by varying the pH (2-10), initial concentration (5-25) mg/L and adsorbent dosage (0.5-2.5) g/L particle size(125-300 μm) and chitosan/graphite mixing ratio (25:75, 50:50 and 75:25). In this preliminary test the effect of one variable was investigated by keeping all the other parameters at constant value.

Table 3.2: Factors and their study level for the OVAT preliminary experiment

Factors	Unit	Levels					
Particle size	µm	125-150	150-250	250-300	300	-	-
Chitosan/graphite mixing ratio	%	25:75	50:50	75:25			
PH	-	2	4	6	8	10	12
Initial on centration of methylene blue dye	mg/L	5	10	15	20	25	-
Adsorbent dosage	g/L	0.5	1	1.5	2	2.5	-
Contact time	minute	30	60	90	120	150	-

3.10. Study of Interaction Effect of Process Parameters and Model Evaluation Using Box-Behnken Design Response Method

The adsorption of methyl blue dye with chitosan/graphite composite adsorbent was carried out in a batch-wise process. Initially, one factor at a time experiment was performed to determine the individual effects of the pH of the solution, adsorbent dosage, initial concentration of methylene blue dye, and contact time. Then the range of the most influential process parameters was chosen depending on the trial result of one factor at a time experiment. By reviewing different literature there are three most influential parameters which affect the adsorption of methylene blue dye. i.e. (Contact time, pH of the solution, and initial concentration). Based on the analysis of one factor at a time experimental data the contact time in the range (of 60-120) minutes, initial concentration of methylene blue dye (5-15) mg/L, and initial solution pH in the range of (6-10) were chosen with three levels each as shown below for further study. Then the interaction effect among study parameters (Initial concentration of methylene blue dye, pH of the solution, and contact time) was studied by using Box-Behnken which is the subset of RSM. The Box-Behnken was used to analyze the experimental data and to determine the optimum process parameters for the efficient removal of methylene blue dye with the adsorbent material. The removal efficiency was related to the independent variable by the quadratic regression mathematical model as shown below

Removal efficiency (%) = $Y = \beta_0 + \beta_1 A + \beta_2 B + \beta_3 C + \beta_{12} AB + \beta_{13} AC + \beta_{23} BC + \beta_{11} A^2 + \beta_{22} B^2 + \beta_{33} C^2 + \varepsilon$ (3)

Where Y is a response variable, β_0 is a constant, A, B, and C are independent variables or the study factors, β_is are the coefficients for the liner interaction effect, $\beta_{ii}s$ are the coefficients for the cross-product interaction effect, $\beta_{ij}s$ are the coefficients for quadratic interaction effects and ε is the random error.

3.10.1. Independent Factors and Their Codded Levels for BBD Experiments

Table 3.3: Independent factors and their coded level for the BBD experiment

Factor	symbol	Units	Levels		
			Low (-1)	Medium(0)	High(+1)
Initial dye concentration	A	mg/L	5	10	15
pH of the solution	B	pH	6	8	10
Contact time	C	minute	60	90	120

In this work, the interaction between process variables (contact time, initial concentration of methylene blue dye, and solution pH) was investigated to develop a mathematical relationship between the dependent and independent variables, or between the operational parameters and response. The interaction effect of three operating factors on the removal effectiveness of chitosan/graphite was investigated: beginning concentration of methylene blue dye (5-15) mg/L, initial pH of the solution (6-10) g/L, and contact time (60-120) min. 17 experiments were carried out, and their effects were investigated, and optimized, and the results were validated (Table 3.4)

3.10.2. Experimental Setup

Table 3.4: BBD design matrix for three factors

Std	Run	A: Initial concentration of dye	B: pH of the solution	C: Contact time	Removal efficiency (%)	
					Actual	Predicted
		mg/L	pH meter	Minute	%	
12	1	10	10	120	85.98	86.03
3	2	5	10	90	97.74	97.71
11	3	10	6	120	74	73.55
6	4	15	8	60	49.59	49.60
9	5	10	6	60	57.96	57.91
2	6	15	6	90	51.42	51.45
10	7	10	10	60	73.02	73.47
7	8	5	8	120	95.95	95.94
14	9	10	8	90	56.79	56.45
13	10	10	8	90	56.5	56.45
16	11	10	8	90	55.98	56.45
17	12	10	8	90	55	56.45
5	13	5	8	60	69.27	68.85
8	14	15	8	120	50.3	50.72
1	15	5	6	90	76.3	76.76
15	16	10	8	90	58	56.45
4	17	15	10	90	59	58.54

As a response, the removal efficiency obtained from the experimental investigation under the interaction impact of the three operational parameters was used. The model's significance was assessed using a statistical analysis tool (ANOVA) in terms of coefficient of determination (R^2), fisher value (F-value), and probability (p-value). Three replicate experiments were carried out, and an average value was calculated.

3.11. Optimization of Process Parameters and Statistical Analysis

Optimization of the process variable (i.e. Contact time, initial concentration of methylene blue dye, and initial solution pH) was conducted using design expert version 13. The removal efficiency, obtained from an experimental study under the interaction effect of the three operating parameters

was used as a response. Triplicate experiments were conducted using optimization parameters and an average value was taken to compare with the predicted one.

3.12. Adsorption Isotherms and Kinetic Studies

The well-known isotherms and kinetic models were examined to study the capacity and the rate of adsorption at which methylene blue dye adsorbed onto chitosan/graphite composite adsorbent.

3.12.1. Adsorption Isotherms

The equilibrium relationship between the amount of methylene blue dye component adsorbed and the one that remains in the solution has been established by using the adsorption equilibrium model. Both Langmuir and Freundlich isotherm models were examined to fit the experimental data. The equilibrium adsorption capacity of methylene blue dye concentration is calculated by equation (Zhang et al., 2011).

$$q_e = \frac{(C_i - C_e) \times V}{m} \tag{3}$$

Where q_e is the amount of adsorbate adsorbed at equilibrium (mg/g), $c_i, c_e, V\ and\ m$ is the initial concentration of methylene blue dye (mg/L), the concentration of methylene blue dye at equilibrium (mg/L), and volume of methylene blue dye solution (L) and mass of adsorbent (g) respectively.

Langmuir Isotherm Model

Langmuir adsorption isotherm deals with the following assumptions

1. Adsorption is taking place in a monolayer homogenous surface of adsorbent of identical sites that are equally available;
2. Molecules are adsorbed at discrete active sites on the surface and the saturation point will reach;
3. Energetically uniform adsorbent surface;
4. No interaction between adsorbate molecules;

The linear form of Langmuir isotherm is given by:-

$$\frac{C_e}{q_e} = \frac{C_e}{q_m} + \frac{1}{q_m k_l} \quad (4)$$

where the values of the Langmuir rate constant K1 L/kg and maximum adsorption capacity $q_m(\frac{mg}{g})$ are obtained from the slope and intercept of $\frac{1}{q_e}\ vs\ \frac{1}{c_e}\ plote$ respectively and $C_e, q_e,$ stands for the equilibrium concentration of MB dye in (mg./l) and mg/g respectively. The maximum theoretical methylene blue dye adsorbed and the Longmuir constant related to the affinity of binding (L/mg) respectively (da Silva Alves et al., 2021).

Freundlich Isotherm Model

The Freundlich isotherm model is derived from the assumption of adsorption taking place on multilayer a heterogeneous adsorption site. It is used to describe non-ideal and reversible adsorption processes. The linear form of Freundlich adsorption isotherm can be formulated as: -

$$lnq_e = lnk_f + \frac{1}{n} lnc_e \quad (5)$$

Where Ce is the concentration of methylene blue dye at equilibrium in the solution, q_e is the amount of methylene blue dye adsorbed at equilibrium, and 1/n shows a more heterogeneous surface which implies that as the value of 1/n approaches one, the adsorbent approaches to the more homogenous binding site. Where the value of the inverse of adsorption intensity 1/n and Fruendlich constant k_f are obtained from the slope and intercept of the $\ln(q_{e)} vs\ \ln(c_e)\ graph$. (A.O, 2012).

3.12.2. Kinetic Studies

The rate of adsorbate uptake and the mechanism of the adsorption process can be studied using pseudo-first-order and pseudo-second-order kinetic models. To investigate the rate of adsorption and controlling mechanism of the adsorption process such as mass transfer and chemical reaction the pseudo-first-order and pseudo-second-order equations were applied to model the kinetic of methylene blue dye adsorption onto chitosan/graphite composite adsorbent.

To study the adsorption of methylene blue dye onto chitosan/graphite composite adsorbent 0.2g of adsorbent was added to 100 ml of methylene blue dye solution with an initial concentration of 10 mg/L in 250ml reaction flask. The solution was stirred at 120 rpm for 30 minutes at room temperature. To investigate the kinetics of the methylene blue dye adsorption process, the adsorbent and adsorbate were contacted by varying the contact time to 60,120 and 180 minutes. At the end of each experiment, the filtrate was analyzed for the final concentration of methylene blue dye using UV visible spectroscopy at a maximum wavelength of 663 nm. The amount of methylene blue dye adsorbed concerning time onto the chitosan/graphite composite was calculated using the equation (Jawad et al., 2021).

$$q_t = \frac{(C_i - C_t) \times V}{m} \tag{6}$$

Where q_t (mg/g) is the amount of methylene blue dye adsorbed at time t, C_i the initial concentration of methylene blue dye (mg/L), C_t (mg/L) the concentration of methylene blue dye in the solution at time t, V (L) is the volume of the solution, and m (g) is the adsorbent dosage.

Pseudo First-Order Kinetic Model

The pseudo-first-order kinetic model assumes that the rate of adsorbate uptake is directly proportional to the number of available active sites in the adsorbent material. The fitness of the pseudo-first-order kinetic model was tested using a linearized formula as shown below in equation **7** (Chang et al., 2016).

$$\ln(q_e - q_t) = ln(q_e) - k_1 t \tag{7}$$

Where k_1(1/min) is the pseudo-first-order rate constant and t is the adsorption time (min). The values of k_1 and $q_e$can be determined from the slope and intercept of the linear plot of $\ln(q_e - q_t)$ versus t respectively.

Pseudo Second-Order Kinetic Model

The pseudo-second-order assumes that the adsorption rate is directly proportional to the concentration of dye. The data used to fit the model are represented using linear as shown in equation 8 shown below.

$$\frac{t}{q_t} = \frac{1}{{q_e}^2 k2} + \frac{1}{q_e} \tag{8}$$

Where is $k2$ ($gmg^{-1}min^{-1}$) is the pseudo-second-order rate constant. The values of $k2$ and q_e can be calculated from the slope and intercept of the $\frac{t}{q_t}\ visrus\ t$ linear plot

4. Result and Discussion

4.1. Effect of Mixing Ratio on Removal Efficiency

The effect of mixing ratio was investigated by varying the mixing ratio in the range of 125-150, 150-250 and 250-300μm keeping constant the PH at 7, initial concentration 10mg/L, adsorbent dosage 1g/L and contact time 60 minutes. The experiment for the chitosan/graphite mixing ratio is illustrated in figure 4.1 below. The experimental result shows that adsorbent material with (chitosan/graphite mixing ratio=75:25) results in an outstanding removal efficiency (67.87%) which was selected for further experiment of the study.

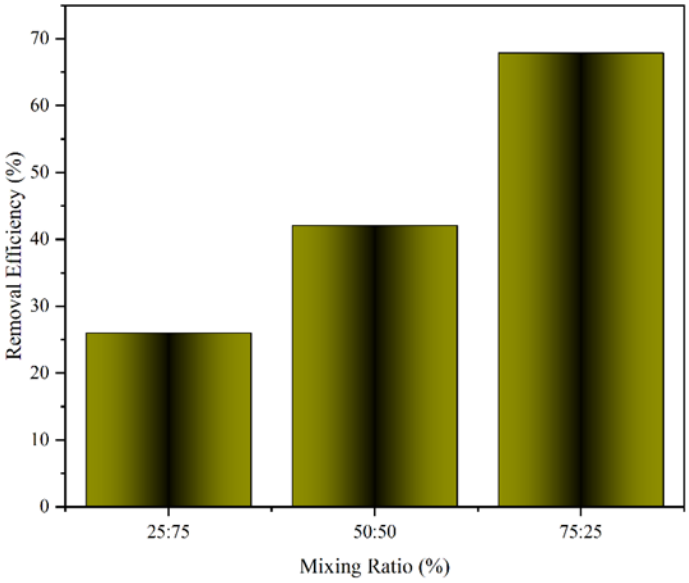

Figure 4.1: Effect of mixing ratio on the removal of methylene blue dye

4.2. Physicochemical Characterization of Graphite, Expanded graphite, and Chitosan/graphite composite adsorbent

4.2.1. Specific Surface Area Analysis

Based on the result of the specific surface area analysis shown in appendix E; graphite, expanded graphite, and chitosan/graphite composite have a specific surface area of 1193.750 m^2/g, 1223.648 m^2/g, and 494.796 m^2/g respectively. The expansion of graphite using the thermal expansion method increases the specific surface area of graphite from 1193.750 to 1223.648 successfully, so based on the analysis result from the BET method and SEM image expanded graphite shows better

surface and pore size which creates suitable conditions for the impregnation of chitosan. As reviewed in many literature, many researchers report low Specific surface area for chitosan. A study conducted (Dongre, 2016) found the specific surface area of chitosan was 12.9.m^2/g. Similarly, a study conducted by (Dongre, 2018) reports the specific surface area of graphite-doped chitosan composite was found 3.90m^2/g with a 176-246 µm particle size range. Another study conducted by (Zhu et al., 2020) reports a specific surface area of chitosan/graphene oxide was 297.431m^2/g. Therefore in the current study, the high specific surface of expanded graphite gives the synthesized chitosan/graphite composite a higher specific surface area which is suitable for adsorption application.

TABLE 4.1: BET texture properties of graphite, expanded graphite, and chitosan/graphite composite

Sample	Surface area (m^2/g)	Cumulative pore volume (m^3/g)
Graphite	1193.750	384.4549
Expanded graphite	1223.648	389.5864
Chitosan/graphite composite	494.796	129.55842

4.2.2. X-Ray Diffraction (XRD) Analysis

The XRD plot of graphite expanded graphite, and chitosan/graphite composite was presented in Figure 4.2 below to see the crystallinity and structural change of the material during the reaction. The XRD plot for graphite shows about 22 number of peaks. The higher diffraction angles were observed at 2θ=26.18 and 2θ=26.08 with 0.334A^o and 0.34A^o corresponding interlayer spacing. The presence of high diffraction intensity in graphite indicates the presence of highly organized crystal stricture. The same result was reported by (Gedam et al., 2015) research conducted on the synthesis and characterization of graphite-doped chitosan composite for batch adsorption of lead (III) ion from aqueous solution. However, after the expansion process, the structural order of graphite was decreased. Most of the peaks including the peak- at 2θ=26.18 disappeared on the XRD pattern of expanded graphite. The disappearance of the diffraction peaks at 2θ=26.18 infers that the expansion process is completed (Ardestani et al., 2022)**.** In figure 4.2 XRD plot for expanded graphite 11 peaks were observed at 2θ=23.66, 23.72, 24.02, 24.1 .24.64, 24.78, 24.96, 25.82, and 26.08. The corresponding spacing of those peaks 0.3755, 0.375, 0.37, 0.368, 0.36,

0.345, and 0.34A^{o} which is higher interlayer space compared to the main diffraction peaks in graphite peaks of graphite at 2θ=26.18 and 2θ=26.08.

The peaks at 26.08 and 26.18 observed on expanded graphite on graphite/ chitosan composite represent the presence of expanded graphite on the composite. Peaks at 2θ=26.2 and 26.28 observed on expanded graphite disappeared on chitosan/graphite composite. This is because of the presence of a lower percentage of expanded graphite on the composite and the reaction of expanded graphite with the amine group of chitosan (Tavakoli et al., 2020).

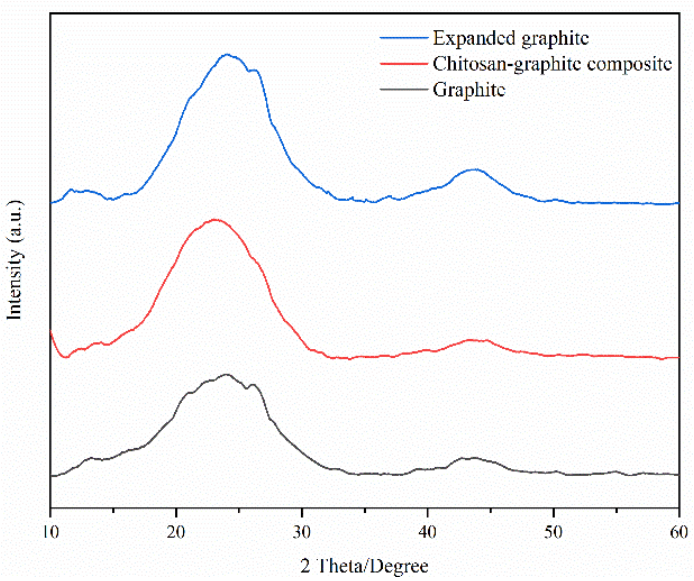

Figure 4.2: XRD diffraction of graphite, expanded graphite, and chitosan/graphite composite

4.2.3. Fourier Transform Infrared Spectroscopy (FTIR) Analysis

The functional group graphite, expanded graphite, and chitosan/graphite composite were analyzed as shown in Figure 4.3 below. The peaks at 2822 cm^{-1} which is in the range of 2850-2920 cm $^{-1}$ on expanded graphite correspond to the stretching vibration of CH2 (Ardestani et al., 2022). Peaks at 2875.4 cm^{-1} on the chitosan/graphite composite graph, which is found in the range of 2800-2950 attributed to the stretching vibration of OH present in chitosan. Peaks at 1482 cm^{-1} and 1588 cm^{-1} attribute to N-H and C-N bond respectively (Dongre, 2018). The peaks in the region from 900-1200 cm^{-1} (at 1051.2, 1090.6, 1138.2, and 1192.4, cm^{-1}) represent the carbohydrate ring of chitosan (Elwakeel et al., 2021). However, in the graph of chitosan/graphite composite accounts

many new peaks appeared due to due to the introduction of amino and hydroxyl groups from chitosan.

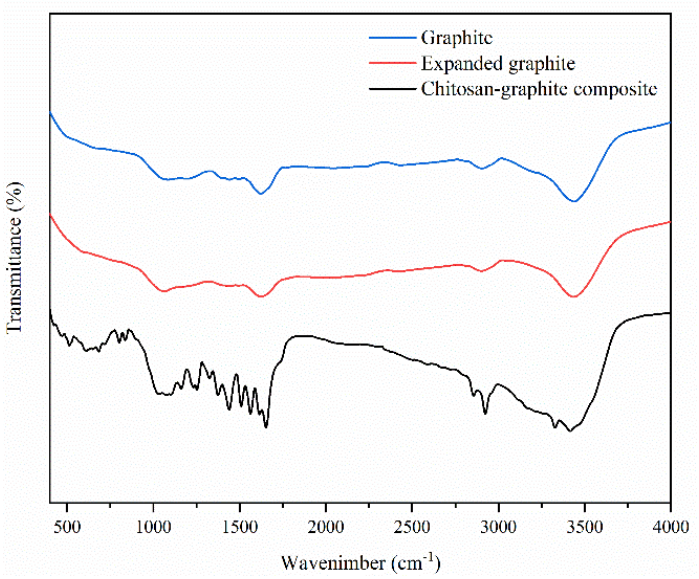

Figure 4.3: FTIR Spectra of graphite, expanded graphite, and chitosan/graphite composite

4.2.4. Scanning Electron Microscope (SEM) Analysis

The surface morphology of the three samples is presented in Figure 4.4 below. As shown in Figure 4.4 below the scanning electron graphite image (a) indicates a smooth surface with less porosity compared to the expanded graphite image (b). Despite this, the scan of expanded graphite shown in the image (b) has a typical texture resulting from the expansion of the bubble gas at high temperatures that makes it suitable for the impregnation of chitosan. In the same fashion, the surface of the chitosan/graphite composite image (c) shows a rough surfaces because some of the pores are blocked during the impregnation of chitosan resulting in the introduction of new functional groups. On the surface of composite adsorbent different regular shape non uniform size pore are observed, which increases the specific surface area as confirmed by BET surface area analysis.

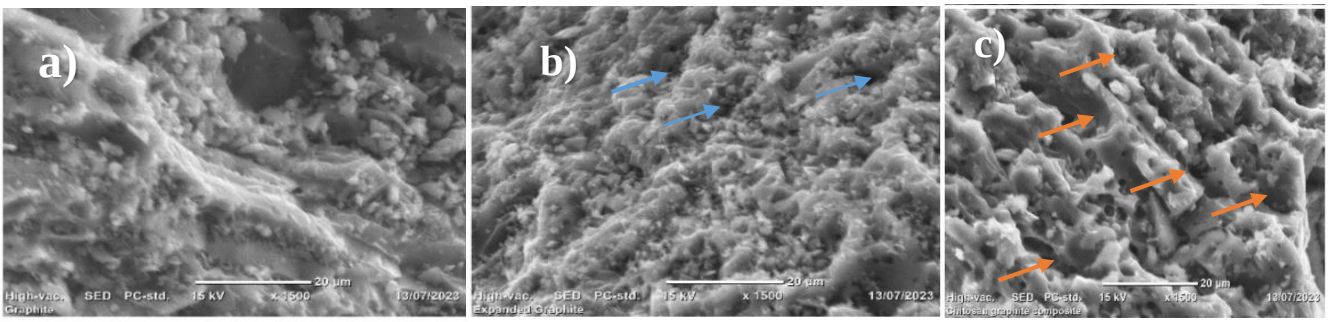

Figure 4.4: SEM image of a). Graphite, b). Expanded graphite and c). Chitosan/graphite Composite

4.2.5. Point of Zero Charge

As shown in Figure 4.5 the PZC is located around 5.8. This indicates that anion adsorption is enhanced at pH less than PZC while pH greater than PZC is preferable for cationic adsorption. Where the point of zero charges is defined as the point at which the surface exhibits net zero charges or the point at which the number of positive and negative charges becomes equal.

The adsorption of cationic is favored when the pH of the solution is greater than the point of zero charge. Those the adsorption of methylene blue dye is promoted at a pH value higher than the point of zero charge. Despite having a net positive charge below the point of zero charge, chitosan/graphite adsorbent exhibits electrostatic repulsion with the positively charged cat ions of methylene blue dye. As shown in Figure 4.5 the PZC is around 5.8 and the adsorbent surface has a net negative charge above this pH value, which increases the removal of methylene blue dye due to the electrostatic force of attraction between the negatively charged adsorbent surface and the positively charged methylene blue cation(Bakatula et al., 2018).

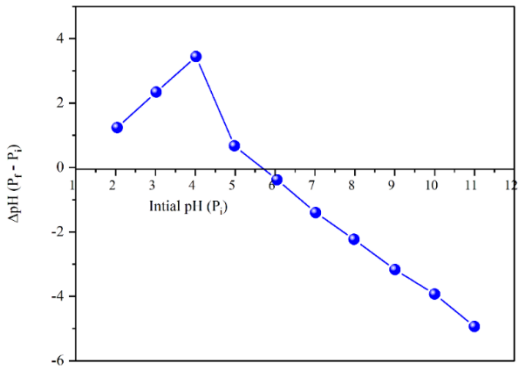

Figure 4.5: Point of zero charge of chitosan/graphite composite

4.3. Adsorption Experiment and Effect of Individual Parameters

4.3.1. Effect of Particle Size

In this study, the effect of particle size on removal of methylene blue dye was investigated by varying the particle size at 125-150,150- 250, and 250-300 µm and at constant initial concentration of 10mg/L, adsorbent dosage 1g/L, pH of 7 and adsorption time of 60 minutes. The experimental result shows that the particle size in the range of (125-150)μm best removal efficiency which is 61.82%. As illustrated in Figure 4.6 below removal efficiency increases as the particle size of the adsorbent material decreases. This is the result of increases in the available surface of the adsorbent with the decrease in particle size (Kannan & Sundaram, 2001).

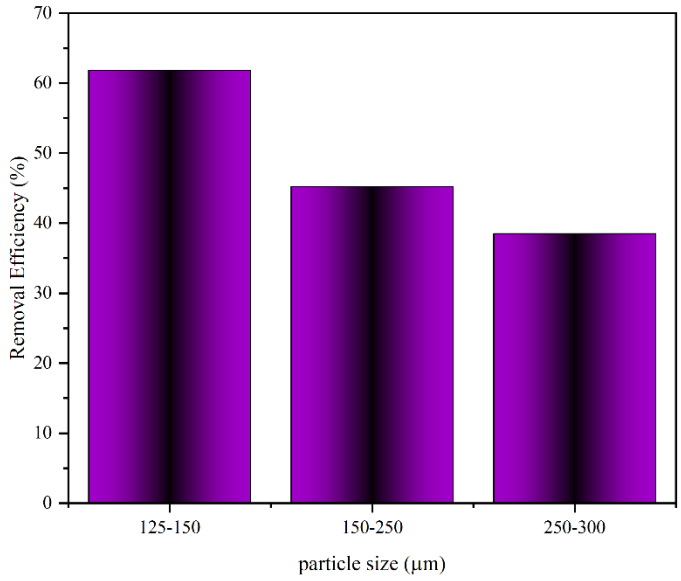

Figure 4.6: Effect of particle size on adsorption of methylene blue dye

4.3.2. Effect of pH of Solution

The initial pH of the solution plays a vital role on adsorption of methylene blue dye with chitosan/graphite composite. In this study, the effect pH on the adsorption of methylene blue dye was performed by varying the solution pH at 2, 4, 6, 8, 10 and 12 and at constant adsorption time 60 minute, adsorbent dosage 1g/L, particle size 125-150 µm initial concentration of and10mg/L.As shown in figure 4.7, the results of the current study show an increment in removal efficiency with increasing the initial pH of the solution as shown in Figure 4.7. The lower removal efficiency was observed at a lower pH (below pH of 6) which proves the results of the point of zero charge

analysis. Increasing the pH of the solution from 6 to 10 increases the removal efficiency from 38.18% to 77.12%. However, a further increment of the pH from 10 to 12 shows a slight increment in removal efficiency i.e. 77.12% to 77.19% which is almost constant. Depending on this preliminary experimental test and point of zero charge analysis a pH range of 6-10 was selected for further studies of interaction effect and optimization in this paper. A research conducted by (Kyzas et al., 2015) supports this study. The increment of removal efficiency with solution pH is due to the fact increase in pH results increase in the concentration of hydroxide ions in the given solution which causes the surface of the adsorbent to deprotonate and become negatively charged. This intern increases the electro force of attraction between the negatively charged chitosan/graphite composite surface and the positively charged methylene blue dye. On the other hand, the lower removal efficiency of the lower pH value is the result of high computation between the hydrogen ions in the solution of lower pH and methylene blue dye for the available active site on the surface of the adsorbent. Several studies also support the best removal efficiency of cationic dyes on basic media. A study conducted by (Song et al., 2022) entitled Preparation and Adsorption Properties of Magnetic Grapheme Oxide Composite for the removal of methylene blue from water supports the current study. The high removal efficiency on basic media makes chitosan/graphite the best alternative adsorbent marital for the removal of methylene blue dye from textile waste water. By reviewing many literature, textile wastewater is basic in normal conditions due to the addition of sodium hydroxide during the dying process (Pekakis et al., 2006).

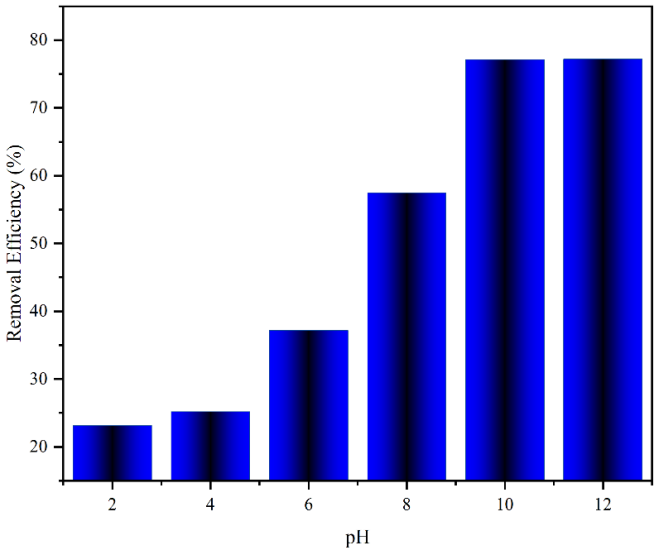

Figure 4.7: Effect of pH on adsorption of methylene blue dye

4.3.3. Effect Adsorbent Dosage

The effect of chitosan/graphite composite dosage on MB removal efficiency was investigated by varying the adsorbent dosage at 0.5, 1, 1.5, 2, and 2.5 mg/L, keeping constant the pH at 10, contact time 60 minute, initial concentration at 10mg/L, and particle size of 125-150 µm. As shown in 4,8 ; the result shows that the removal efficiency increases sharply with an increase in the adsorbent dosage from 0.5g/L to 1g/L which indicates the presence of more MB molecules for further adsorption, however Further increment from 1g/L to 2g/L increases the removal efficiency slightly and it becomes almost constant as the dosage increases from 2g/L to 2.5g/L, which suggests that the majority of methylene blue dye are adsorbed and only negligible amount of concentration remains on the solution(Ghosh et al., 2021). As a result, 2g/L was chosen as the maximum value for further studies. A research conducted by (Labidi et al., n.d.) entitled “functional chitosan derivative and chitin as decolonization materials for methylene blue and methylene orange from the aqueous solution” has shown similar patter and supports this study.

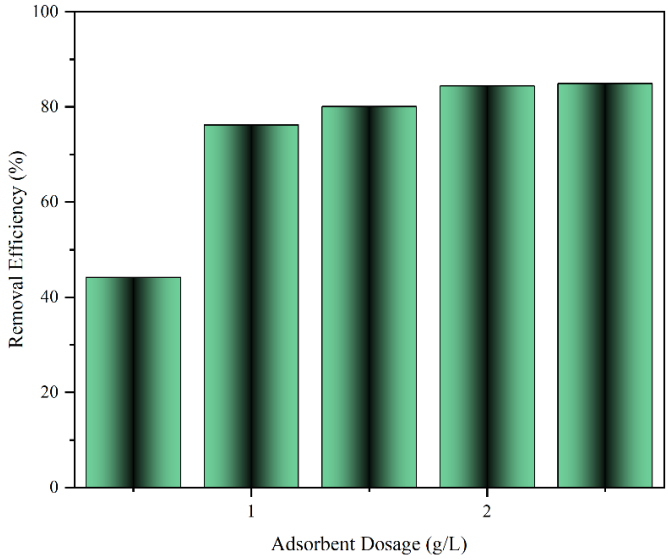

Figure 4.8: Effect of adsorbent dosage on adsorption of methylene blue dye

4.3.4. Effect of Initial Concentration of Methylene Blue Dye

The effect of initial concentration of methylene blue dye is another basic factor which affects the adsorption process. The effect initial concentration on the adsorption of methylene blue dye using chitosan/graphite composite was studied by varying the concentration at 5, 10, 15 and 20 mg/L and keeping constant pH at 10, contact time 60 minute, adsorbent dosage 2g/L, and particle site 125-150µm. As shown in Figure 4.9, the removal efficiency decreases from 81.91 to 77.4 % as the initial concentration of methylene blue dye increases from 5 mg/L to 10 mg/L. This is because, at the lower initial concentration of methylene blue dye, the ratio of methylene blue dye molecules to the available active adsorption site is low, which enhances the removal efficiency. As shown in Figure 4.9 below the removal efficiency decreases slightly as the initial concentration increases from 5mg/L to 10 mg/L, but the father increment of initial concentration of methylene blue dye after 10mg/L results in a rapid decrease in adsorption of methylene blue dye. This is because, at the higher initial concentration of methylene blue dye, the ratio of methylene blue dye molecules to the available active site is high which affects the adsorption capacity negatively.

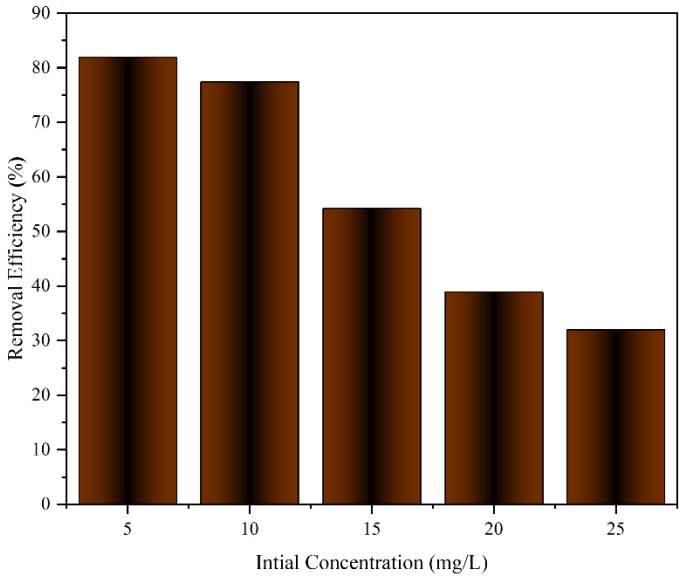

Figure 4.9: Effect of initial concentration on adsorption of methylene blue dye

4.3.5. Effect of Contact Time

The effect of contact time on adsorption of methylene blue dye using Chitosan/Graphite composite was investigated by varying the contact time at 30, 60, 90, 120 and 150 minutes keeping constant the pH at 10, initial concentration 10 mg/L adsorbent dosage 2g/L and particle size 125-150µm. The removal efficiency increases sharply for the first 30 minutes as the time increases from 30 to 60 minutes. This rapid increase in removal efficiency indicates the availability of unoccupied active sites. Removal efficiency increases slightly as the time increases from 60 to 120 minutes. This indicates the lack of available active sites on the surface of the adsorbent. The optimum removal efficiency was obtained after 90 minutes. The removal efficiency at 120 and 150 contact time was 85.98 and 86.8 respectively which is very similar and further increment in contact time doesn't show a significant increment in removal efficiency and 120 minutes was taken as equilibrium time. The rapid increment of removal efficiency with contact time in the first few minutes is due to the presence of a large number of the free active sites for adsorption, and as time goes the number of unoccupied sites decreases and a repulsive force is developed due to between the solid particle present on the surface of the adsorbent and in the bulk solution which results from gradual slowdown and finally equilibrium time is reached (A. Ahmad et al., 2009).

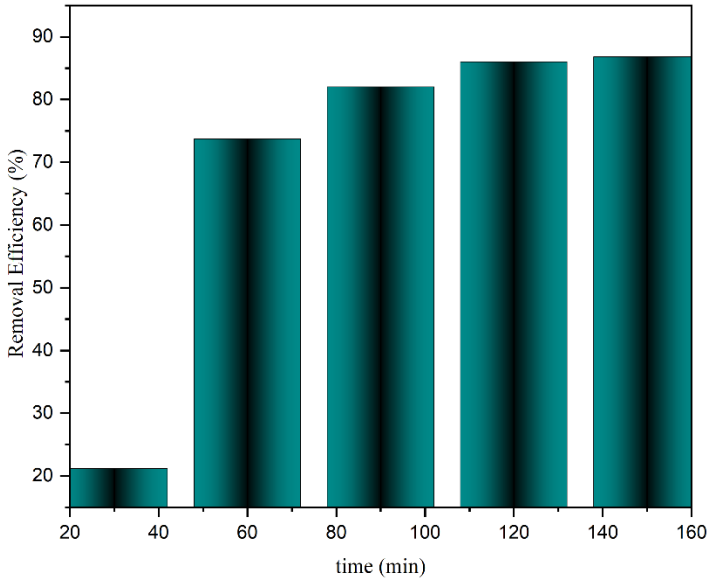

Figure 4.10: Effect of contact time on adsorption of methylene blue dye

4.4. Statistical Analysis and Adsorption Performance

4.4.1. Sequential Model Sum of Squares

The validity of the model that was developed to connect the study variable and response was evaluated by the correlation coefficient (R^2), which is closer to unity as a result of the predicted value for the response being closer to the actual value, as shown in table 4.2 Regression calculations were performed to fit all of the polynomial models to the specified response. Furthermore, the impacts of all model terms are compared using statistical measures like the sum of squares, F-values, and p-values. As a result, the response function was predicted using the recommended second-order regression function. After examination, the quadratic model function was found to be statistically significant with an R^2 Value of 0.9931 as shown in Table 4.2 for the response. This is based on the selection of the highest-order polynomial where the addition of terms is significant and the model is not aliased.

Table 4.2: Sequential model sum of squares

Source	Sum of squares	df	Mean square	F-value	P-value	
Mean vs Total	74157.64	1	74157.64			
Linear vs Mean	2868.83	3	956.28	12.85	0.0003	
2FI vs Linear	219.01	3	73.00	0.9756	0.4423	
Quadratic vs 2FI	**742.26**	**3**	**247.42**	**287.53**	**< 0.0001**	**Suggested**
Cubic vs Quadratic	1.18	3	0.3932	0.3247	0.8088	Aliased
Residual	4.84	4	1.21			
Total	77993.76	17	4587.87			

4.4.2. Analysis of variance (ANOVA)

The model's significance was assessed using a statistical analysis tool (ANOVA) in terms of coefficient of determination (R^2), fisher value (F-value), and probability (p-value), as shown in Table 4.3. A model with a P value less than 0.05 and an R^2 value close to unity is the best-fitted model. In this aspect, the model F-value of 494.56 indicates that the model is significant. An F-value this large is just 0.01% likely to occur due to noise.

Model terms are significant if the P-value is less than 0.05%. A, B, C, AB, AC, A^2, B^2, and C^2 are significant model terms in this scenario with (P-value 0.05) at 95% confidence. The lack of fit F-value of 0.32 indicates that the lack of fit is insignificant in comparison to pure error. There is an 80.88% likelihood that this big lack of fit F- value is due to noise. The non-significant lack of fit is positive and demonstrates the developed model.

Similarly, the effect and significance of the main factors and interaction variables were statistically analyzed using statistical P-value and F-value parameters as shown in the ANOVA table, which shows that all of the main factors (initial concentration, pH of the solution, and contact time) are

significant with P-value 0.0001 and interactive factors of AB and AC with P-value less than 0.0001. As seen in Table 4.3, all quadratic terms were significant with P-values of 0.0001.

Table 4.3: Analysis of variance (ANOVA) table

Source	Some of Square	Df	Mean square	F-value	P-value	
Model	3830.10	9	425.57	494.56	< 0.0001	Significant
A-Initial concentration of dye	2078.51	1	2078.51	2415.47	< 0.0001	
B-PH of the solution	392.84	1	392.84	456.53	< 0.0001	
C-Contact time	397.48	1	397.48	461.92	< 0.0001	
AB	48.02	1	48.02	55.81	0.0001	
AC	168.61	1	168.61	195.94	< 0.0001	
BC	2.37	1	2.37	2.76	0.1408	
A^2	70.75	1	70.75	82.22	< 0.0001	
B^2	469.69	1	469.69	545.83	< 0.0001	
C^2	137.97	1	137.97	160.33	< 0.0001	
Residual	6.02	7	0.8605			
Lack of Fit	1.18	3	0.3932	0.3247	0.8088	not significant
Pure Error	4.84	4	1.21			
Cor Total	3836.13	16				

The anticipated and modified coefficients of determinants (R^2-Values) were used to assess the fit of the experimental data to the established regression model. The expected R^2 was found to be 0.9931, which agrees with the modified R^2 of 0.9964. In other words, the difference is smaller than 0.2. This means that the chosen model can explain 99.64% of the overall variation in methylene blue dye adsorption data. The signal-to-noise ratio is measured by the adequacy precision. As stated in Table 4.4, a ratio greater than four is preferable. The signal-to-noise ratio of 67.613 implies that the fitness of a quadratic model can be employed to navigate the design space.

Table 4.4: Fit statics

Std. Dev.	0.9276	**R^2**	0.9984
Mean	66.05	**Adjusted R^2**	0.9964
C.V. %	1.40	**Predicted R^2**	0.9931
		Adeq. Precision	67.6127

The developed mathematical model correlates operating process variables with a response, namely (contact duration, beginning concentration of methylene blue dye in solution, and initial pH of solution) to the percentage of removal efficiency. In this regard, the quadratic model was found to have the best match from those provided by design experts, with P-value 0.0001 and R^2=9931, indicating that the model is significant. In equation 9, the condense quadratic model equation developed by design expert application is given, which relates the response (percentage of chitosan/graphite composite removal efficiency) to the independent process variables (initial pH of the solution, initial concentration of methylene blue dye, and contact time).

$$\text{Removal efficiency } (\%) = +56.45 - 16.12A + 7.01B + 7.05C - 3.47AB - 6.49AC + 4.10A^2 + 10.56B^2 + 5.72C^2 \quad (9)$$

Where A is the initial concentration of methylene blue dye (mg/L), B is the initial PH of the solution and, C is contact time in minute.

The condensed form of the quadratic equation above describes the effect of individual (linear and quadratic) and double interaction variables on the removal of methylene blue dye with chitosan/graphite composite. A variable with a negative coefficient affects the removal efficiency negatively (removal efficiency decreases with increasing the given term), on the other hand, variables with a positive coefficient affect removal efficiency positively (the removal efficiency increases in increasing of given variable). Concerning this initial concentration of methylene blue dye, and double interaction of the initial concentration and pH of the solution affects the removal efficiency negatively and all the other individual interactions affect the removal efficiency positively as shown in equation 9 above.

Diagnostic plots

The models' adequacy was tested by creating several diagnostic plots, as illustrated in Figures 4.11 and 4.12, to determine whether the model equations would provide sufficient approximation values

to the real values. The points on the normal% probability plot of residuals for the responses were reasonably close to the straight line and showed no variance deviation (Figure 4.11). Internally studentized residual plots were also created to aid in the satisfactory fit of the established models, and the plots (Figure 4.12) demonstrate that all of the data points fall within the limits.

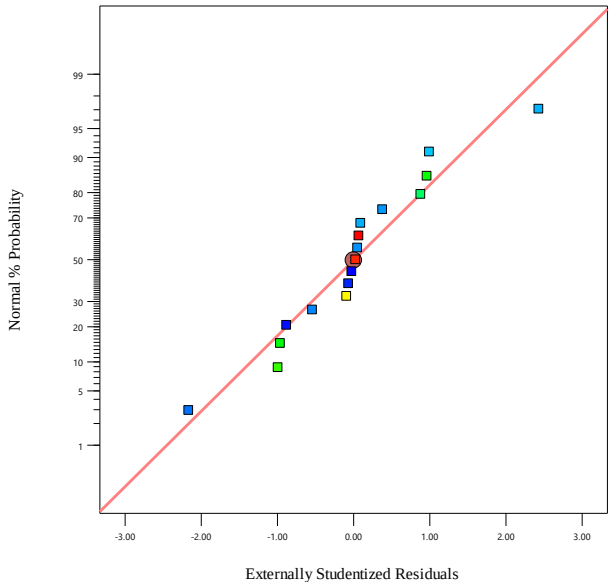

Figure 4.11: Normal plot of residual for removal efficiency

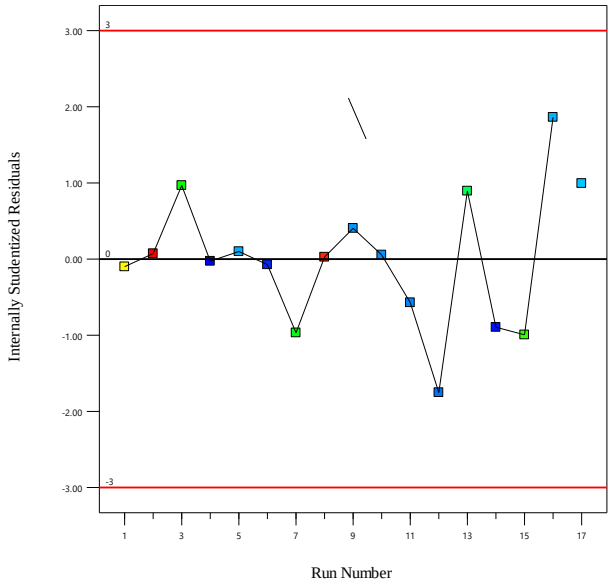

Figure 4.12: Residual versus run for removal efficiency

The projected values from the created models were pretty similar to the experimental values, lie reasonably close to the straight line, and show adequate agreement with the real data (Figure 4. 13).

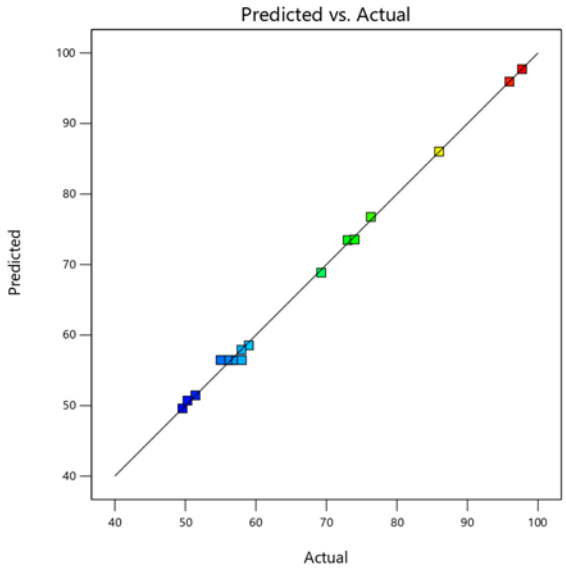

Figure 4.13: Predicted VS Actual Plot for Removal Efficiency

4.4.3. Combined Effect of Process Parameters

Using the BOX-Behnken design (BBD), the influence of process parameters (contact duration, beginning pH of the solution, and initial concentration of methylene blue dye) on methylene blue dye removal was examined. Figure 4.14 a, b, and c show the interaction effect of two process variables on removal efficiency while maintaining the other operation variables constant. Figure 4.14 (a) depicts the interaction effect of the initial methylene blue dye concentration and initial pH of the solution at a constant contact time of 90 minutes. As shown in the 3D plot from Figure 4.14, (a) the removal efficiency increases as the pH increases from 6 to 10 and the initial methylene blue dye concentration decreases from 15mg/l to 5 mg/L. The removal efficiency increase with pH because at higher pH the deprotonated and becomes negative and a force of attraction develops between the negative surface and the positively charged methylene blue dye molecules. Increasing in initial concentration of methylene blue dye due to the presence of limited active sites at 2g/L adsorbent dosage adsorbent. As indicated from the codded model equation of response surface; the combined effect of initial concentration of methylene blue dye and initial solution PH affects

the removal efficiency negatively with coefficient of -3.47 as shown from equation 9 and it has significant effect with p value of less than 0.0001in table 4.3.

Figure 4.14 (b) depicts the combined effect of contact time and initial concentration of methylene blue dye at a constant pH of 10. The elimination of methylene blue dye increases when the contact duration increases from 60 to 120 minutes and the initial concentration of methylene blue dye drops from 15 mg/L to 5 mg/L, as shown by the 3D plot. The removal of methylene blue dye decreases as the initial concentration of methylene blue dye increases from 5 mg/L to 15mg/L because of the presence of limited active site on the surface of the adsorbent of 2g/L dosage. The interaction effect of contact time affects the removal efficiency negatively with coefficient of -6.49 from the as shown in equation 9. It has significant effect with p value less than 0.0001 as summarized in table 4.3.

Figure 4.14 (c) depicts the combined influence of initial solution pH and contact time on methylene blue dye removal effectiveness. It was discovered that increasing the initial pH of the solution from 6 to 10 and increasing the contact period from 60 to 120 minutes improved the removal efficiency. This is supported by the generated model equation, which has a negative e coefficient of 0.7700, as shown in equation 9.

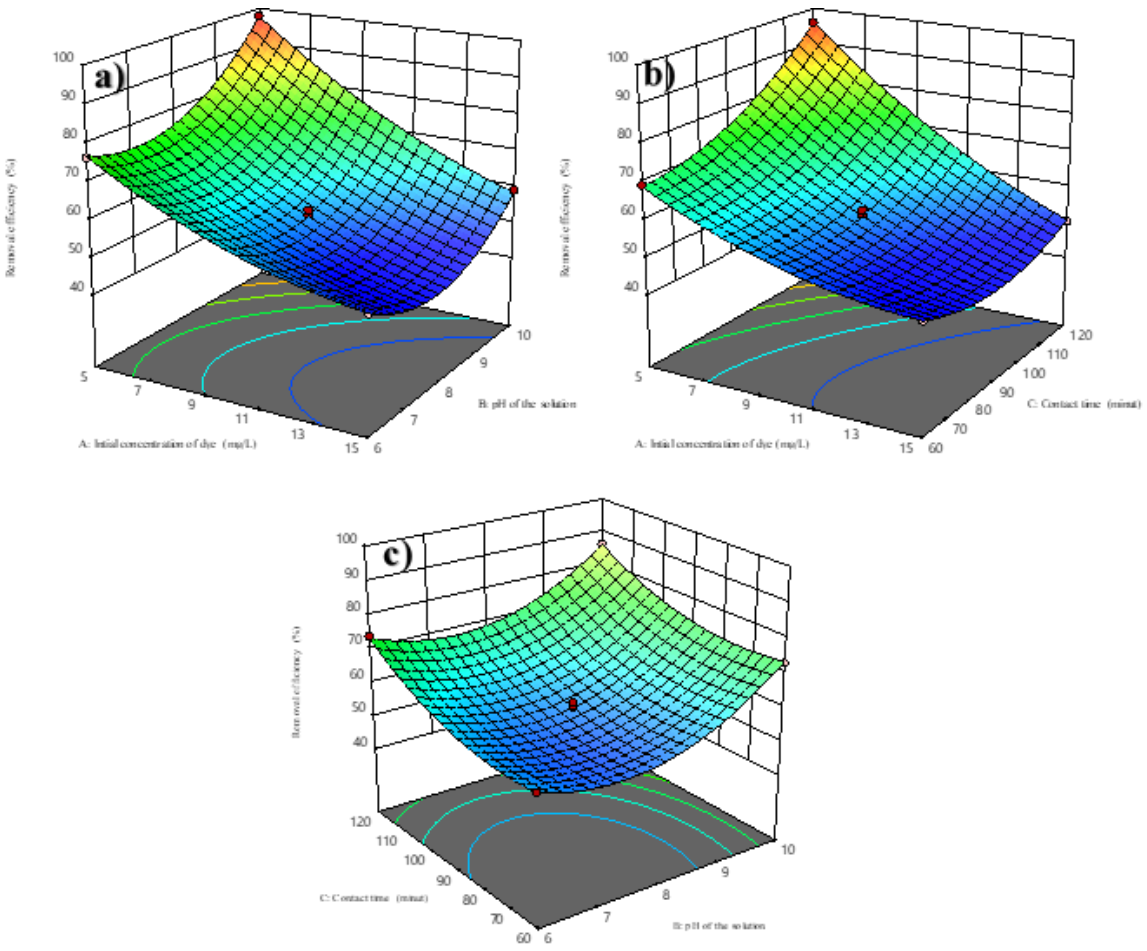

Figure 4.14: Interaction effect of a).pH VS initial concentration, b).Contact time VS initial concentration, C). Contact time VS pH

4.4.4. Statistical Optimization of Process Variables

After the study of the interaction effect of operating parameters, statistician optimization of those process parameters was carried out to investigate the optimum condition for efficient adsorption of methylene blue dye onto chitosan/graphite composite adsorbent. As shown above, the interaction effect of removal efficiency of the adsorbent material increases with increasing contact time, and solution pH and decreases with increasing initial concentration of MB dye. Therefore, such type of fluctuation should be optimized to get the best removal efficiency in the optimum operating conditions. The optimum process conditions were selected based on the high value of the removal efficiency from the given set of solutions generated from design expert software.

Table 4.5: Working condition of factor and response for optimization

Name	Goal	Lower limit	Upper limit
A: Initial concentration of dye	is in range	5	15
B: pH of the solution	is in range	6	10
C: Contact time	is in range	60	120
Removal efficiency	maximize	49.59	97.74

As a result, an initial concentration of 5.24 mg/L, pH of 9.98, and contact time of 95.43 minutes was chosen for maximal methylene blue dye removal of 98.61%. The triplet experiment was carried out to test the optimum results anticipated by the model at the optimum conditions discovered through numerical optimization. The actual removal efficiency obtained from the experiment was in close agreement with the expected value, with a 1.433% variance.

Table 4.6: The model predicted and observed response of optimization

Factors	Initial concentration (mg/L)	pH	Contact time (min)	Removal efficiency (%)
Predicted	5.24	9.98	95.43	98.61
Observed	5	10	96	98.62333

4.5. Adsorption Isotherm and Kinetic Studies

4.5.1. Adsorption Isotherms

In the current study, methylene blue dye adsorption characteristics of chitosan/graphite composite adsorbent were investigated by using both Langmuir and Freundlich adsorption isotherms. Where adsorption isotherm is a mathematical model that determines the distribution of methylene blue dye between the chitosan/graphite composite adsorbent and the mother liquor. To study the adsorption isotherm of methylene blue dye, experiments were conducted on different concentrations of methylene blue dye (5mg/L, 10mg/L, and 15mg/L and 20mg/L) onto chitosan/graphite composite adsorbent. Then the final and equilibrium concentrations as well as the removal efficiency of chitosan/graphite were evaluated. To test the fit of the Langmuir model $\frac{C_e}{q_e}$ versusC_e was plotted as shown in Figure 4.15 (A) below. Then the coefficient of the determinant (R^2), the Langmuir equilibrium constant ($K_L, L/mg$), and maximum adsorption capacity ($q_{max}, mg/g$) were determined from the curve and summarized in Table 4.7. The Langmuir plot in Figure 4.15 (A) has an R^2 value of 0.99612 with slope and intercept values of 0.01019 and 0.11967 respectively.

In the same manner, the model fit for Freundlich was tested by plotting $\ln(C_e)$ versus $\ln(q_e)$ data's at equilibrium. Then the coefficient of the determinant (R^2), Freundlich constant (K_f), and the adoption intensity (n) were determined from the plot in Figure 4.15 (B). As shown in Figure 4.15(B) below the Freundlich plot has 0.95486 R^2 with 0.25348 and 1.4436 slop and intercept values respectively.

Concerning the results obtained from the adsorption isotherm for methylene blue dye of adsorbent the coefficient of determinant by Langmuir ($R^2 = 0.99612$) and coefficient of determinant for Freundlich ($R^2 = 95486$). The coefficient of determinant found by Langmuir is higher than that of Freundlich. From this, we can conclude that the monolayer surface is much more effective than that of the heterogonous layer in the adsorption process. And the maximum removal efficiency is found to be 98.6 mg/g.

The Freudlich parameter n indicates the favorability and intensity of the adsorbent adsorbate system. As illustrated in table **4.7** below the value of 1/n for removal of methylene blue dye with

chitosan/graphite composite is found to be 0. 2535 with (n=3.944). As reviewed in many kinds of literature n> 1 indicates the physical adsorption process and n<1 indicates the chemical adsorption process. As a result, the adsorption of methylene blue dye with chitosan/graphite composite is a physical adsorption process. In addition to this n value between 1 and 10 indicates a favorable adsorption process and a 1/n value between 0.1 and 0.5 indicates an excellent adsorption process (El-Shazly et al., 2021).

Table 4.7: Parameters of isotherm for MB dye adsorption onto chitosan/graphite composite

Isotherm	Parameters	Values
	q_{max} ,(mg/g)	98.135
Langmuir	R_L	0.855
	$K_L, (L/mg)$	0.085
	R^2	0.99612
		1/n=0.2535
Freundlich	K_f	4.235
	R^2	0.95486

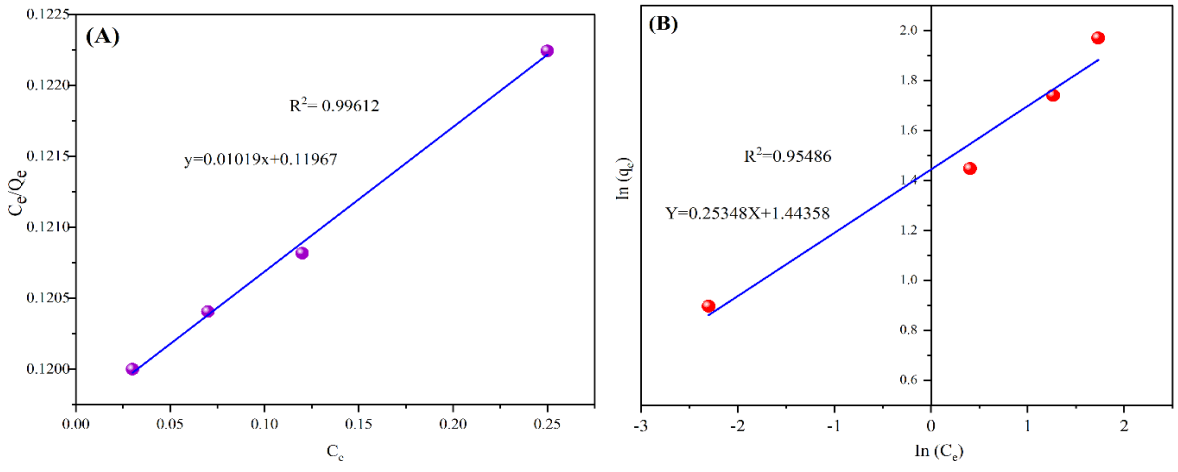

Figure 4.15: Langmuir (A) Freundlich (B) models for methylene blue dye adsorption using chitosan/graphite composite

4.6. Study of Adsorption Kinetics

Both pseudo-first-order and pseudo-second-order kinetic models were tested to study the kinetics of methylene blue adsorption onto chitosan/graphite composite. The fit for the pseudo-first-order kinetic model was examined from $\ln(q_e - q_t)\ uersuss$ adsorption time (t) plot to fit the data. The coefficient of the determinant (R^2) for the pseudo-first-order kinetic model is found to be 0.89227 as shown in Figure 4.16 (A) below. In the same manner, the model fit for pseudo-second-order was investigated from $\frac{t}{q_t}\ visrus\ t$ plot. As shown in Figure 4.16 (B) below the coefficient of the determinant for the pseudo second-order kinetic model is 0.99478. In comparison with pseudo-first-order kinetics, pseudo-second order accounts high coefficient of determinant. From those results, it can be concluded that the adsorption of methylene blue dye onto chitosan/graphite composite follows second-order kinetics.

Table 4.8: Kinetic model parameters for adsorption of MB dye onto chitosan/graphite composite

Kinetic model	Parameters	Value
Pseudo-first-order	$q_{e\ \text{cal}}$,(mg/L)	7.72
	K_1	-3.75× 10^{-5}
	R^2	0.89227
Pseudo-second-order	$q_{e\ \text{cal}}$,(mg/L)	1.033
	K_2	0.0378
	R^2	0.99478

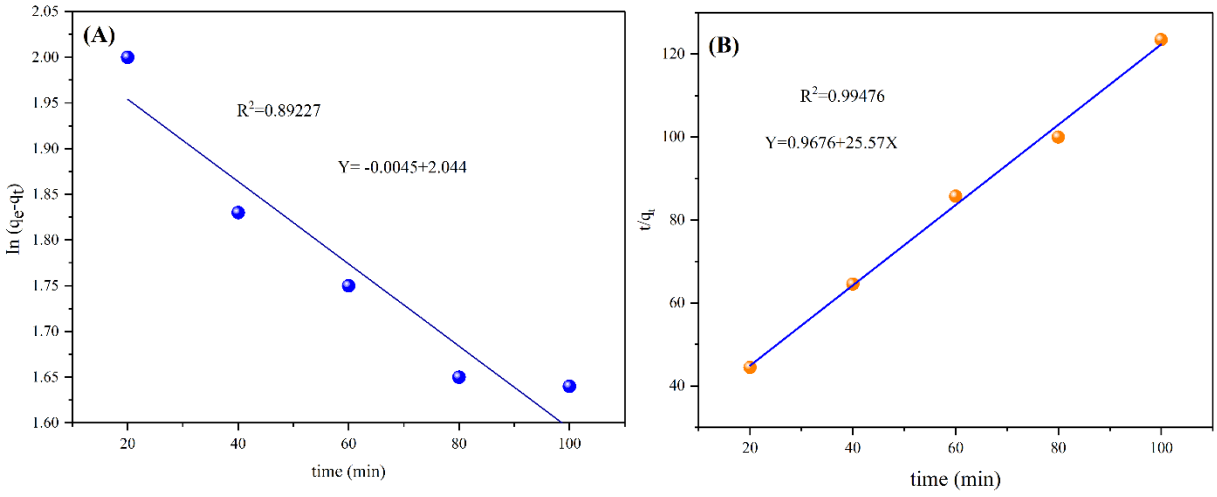

Figure 4.16: Pseudo-first order (A) and pseudo-second-order (B)

5. Conclusion and Recommendation

5.1. Conclusion

A natural chitosan/graphite composite was synthesized using the impregnation method and thermal expansion method. A 75:25 chitosan/graphite mixing ratio was chosen for adsorption experiments. The composite exhibited important adsorbent properties, as demonstrated by BET, FTIR, SEM, and XRD. A preliminary experiment was conducted to investigate the range of operating parameters, including initial pH, adsorbent dosage, contact time, and methylene blue dye concentration. Three factors were selected and optimized using Box-Behnken (BBD) design. A mathematical model equation was developed, showing that the applied process parameters significantly affect the removal of methylene blue dye with the chitosan/graphite composite. The optimum adsorption removal efficiency was achieved at a pH of 9.988, 95.435-minute contact time, and 5.243 mg/L initial methylene blue dye concentration. The composite was found to be the best alternative adsorbent for removing methylene blue dye from textile wastewater.

5.2. Recommendation

In this study chitosan/graphite composite was synthesized and tested to remove methylene blue dye from synthesis wastewater batch-wise. From this point of view for further studies, the following points must be taken into account.

The adsorption of methylene blue dye was conducted using synthetic water batch-wise, but the synthesis wastewater does.t contain other pollutants that can affect the adsorption process such as other dye staff and heavy metals. Therefore, it is recommended to use real industrial methylene blue dye-loaded wastewater effluent for more real and effective investigation.

In addition to this for industrial scale-up and to observe the effect of contact time the adsorption process should be performed in the bed of continuous columns rather than the batch-wise process. Moreover, studies concerning desorption and regeneration and the study of thermodynamics should be conducted to affirm the maximized recovery potential of the composite adsorbent.

Furthermore, separation of the chitosan/graphite composite should be performed using the magnetic separation method by introducing ferromagnetic materials like iron in the composite.

Further study can be needed to study the reusability of the adsorbent material

The economic feasibility of the adsorbent material should be studied.

References

A.O, D. (2012). Langmuir, Freundlich, Temkin and Dubinin–Radushkevich Isotherms Studies of Equilibrium Sorption of Zn 2+ Unto Phosphoric Acid Modified Rice Husk. *IOSR Journal of Applied Chemistry*, *3*(1), 38–45. https://doi.org/10.9790/5736-0313845

Abdelfatah, A. M., Fawzy, M., Eltaweil, A. S., & El-Khouly, M. E. (2021). Green Synthesis of Nano-Zero-Valent Iron Using Ricinus Communis Seeds Extract: Characterization and Application in the Treatment of Methylene Blue-Polluted Water. *ACS Omega*, *6*(39), 25397–25411. https://doi.org/10.1021/acsomega.1c03355

Adel, M., Ahmed, M. A., & Mohamed, A. A. (2021). A facile and rapid removal of cationic dyes using hierarchically porous reduced graphene oxide decorated with manganese ferrite. *FlatChem*, *26*(December 2020), 100233. https://doi.org/10.1016/j.flatc.2021.100233

Agboola, O., Fayomi, O. S. I., Ayodeji, A., Ayeni, A. O., Alagbe, E. E., Sanni, S. E., Okoro, E. E., Moropeng, L., Sadiku, R., Kupolati, K. W., & Oni, B. A. (2021). A review on polymer nanocomposites and their effective applications in membranes and adsorbents for water treatment and gas separation. *Membranes*, *11*(2), 1–33. https://doi.org/10.3390/membranes11020139

Ahmad, A., Rafatullah, M., Sulaiman, O., Ibrahim, M. H., & Hashim, R. (2009). Scavenging behaviour of meranti sawdust in the removal of methylene blue from aqueous solution. *Journal of Hazardous Materials*, *170*(1), 357–365. https://doi.org/10.1016/j.jhazmat.2009.04.087

Ahmad, R., & Ansari, K. (2021). Comparative study for adsorption of congo red and methylene blue dye on chitosan modified hybrid nanocomposite. *Process Biochemistry*, *108*(May), 90–102. https://doi.org/10.1016/j.procbio.2021.05.013

Al-Graiti, W., & Merdas, S. M. (2023). Evaluation of Some Eco-Friendly Food Residues for Removal of Methylene Blue Dye from Aqueous Solutions. *Journal of Medicinal and Chemical Sciences*, *6*(5), 1044–1054. https://doi.org/10.26655/JMCHEMSCI.2023.5.10

Amar, I. A., Sharif, A., Ali, M., Alshareef, S., & Altohami, F. (2020). Removal of Methylene Blue from Aqueous Solutions using Nano-Magnetic Adsorbent Based on Zinc-Doped Cobalt Ferrite. *Chemical Methodologies*, *4*(1), 1–18.

https://doi.org/10.33945/sami/chemm.2020.1.1

Ardestani, M. M., Mahpishanian, S., Rad, B. F., Janmohammadi, M., & Baghdadi, M. (2022). Preparation and characterization of room-temperature chemically expanded graphite: Application for cationic dye removal. *Korean Journal of Chemical Engineering*, *39*(6), 1496–1506. https://doi.org/10.1007/s11814-022-1084-5

Arunachalam, K. D. (2021). Bio-adsorption of methylene blue dye using chitosan-extracted from Fenneropenaeus indicus shrimp shell waste. *Journal of Aquaculture & Marine Biology*, *10*(4), 146–150. https://doi.org/10.15406/jamb.2021.10.00316

Bakatula, E. N., Richard, D., Neculita, C. M., & Zagury, G. J. (2018). Determination of point of zero charge of natural organic materials. *Environmental Science and Pollution Research*, *25*(8), 7823–7833. https://doi.org/10.1007/s11356-017-1115-7

Barus, D. A., Humaidi, S., Ginting, R. T., & Sitepu, J. (2022). Enhanced adsorption performance of chitosan/cellulose nanofiber isolated from durian peel waste/graphene oxide nanocomposite hydrogels. *Environmental Nanotechnology, Monitoring and Management*, *17*(October 2021), 100650. https://doi.org/10.1016/j.enmm.2022.100650

Belachew, N., & Hinsene, H. (2022). Preparation of Zeolite 4A for Adsorptive Removal of Methylene Blue: Optimization, Kinetics, Isotherm, and Mechanism Study. *Silicon*, *14*(4), 1629–1641. https://doi.org/10.1007/s12633-020-00938-9

Chang, J., Ma, J., Ma, Q., Zhang, D., Qiao, N., Hu, M., & Ma, H. (2016). Adsorption of methylene blue onto Fe3O4/activated montmorillonite nanocomposite. *Applied Clay Science*, *119*, 132–140. https://doi.org/10.1016/j.clay.2015.06.038

Chouhan, D., & Mandal, P. (2021). Applications of chitosan and chitosan based metallic nanoparticles in agrosciences-A review. *International Journal of Biological Macromolecules*, *166*, 1554–1569. https://doi.org/10.1016/j.ijbiomac.2020.11.035

da Silva Alves, D. C., Healy, B., Pinto, L. A. d. A., Cadaval, T. R. S., & Breslin, C. B. (2021). Recent developments in Chitosan-based adsorbents for the removal of pollutants from aqueous environments. *Molecules*, *26*(3). https://doi.org/10.3390/molecules26030594

Dbik, A., Messaoudi, N. El, Bentahar, S., Khomri, M. El, Lacherai, A., & Faska, N. (2022). Optimization of methylene blue adsorption on agricultural solid waste using box–behnken

design (BBD) combined with response surface methodology (RSM) modeling. *Biointerface Research in Applied Chemistry*, *12*(4), 4567–4583. https://doi.org/10.33263/BRIAC124.45674583

Dongre, R. S. (2016). Adsorption of hexavalent chromium by graphite-chitosan binary composite. *Bulletin of Materials Science*, *39*(3), 865–874. https://doi.org/10.1007/s12034-016-1200-4

Dongre, R. S. (2018). Benign Graphite-Chitosan Blended Bio-Composite for Sorption of Toxic Nitrate from Water. *Journal of Membrane Science & Technology*, *8*(3), 1–10. https://doi.org/10.4172/2155-9589.1000189

Doondani, P., Jugade, R., Gomase, V., Shekhawat, A., Bambal, A., & Pandey, S. (2022). Chitosan/Graphite/Polyvinyl Alcohol Magnetic Hydrogel Microspheres for Decontamination of Reactive Orange 16 Dye. *Water (Switzerland)*, *14*(21). https://doi.org/10.3390/w14213411

El-Habacha, M., Dabagh, A., Lagdali, S., Miyah, Y., Mahmoudy, G., Sinan, F., Chiban, M., Iaich, S., & Zerbet, M. (2023). An efficient and adsorption of methylene blue dye on a natural clay surface: modeling and equilibrium studies. *Environmental Science and Pollution Research*. https://doi.org/10.1007/s11356-023-27413-3

El-Shazly, E. A. A., Dakroury, G. A., & Someda, H. H. (2021). Kinetic and isotherm studies for the sorption of 134Cs and 60Co radionuclides onto supported titanium oxide. *Journal of Radioanalytical and Nuclear Chemistry*, *330*(1), 127–139. https://doi.org/10.1007/s10967-021-07956-w

Eltaweil, A. S., Elgarhy, G. S., El-Subruiti, G. M., & Omer, A. M. (2020). Carboxymethyl cellulose/carboxylated graphene oxide composite microbeads for efficient adsorption of cationic methylene blue dye. *International Journal of Biological Macromolecules*, *154*, 307–318. https://doi.org/10.1016/j.ijbiomac.2020.03.122

Elwakeel, K. Z., Elgarahy, A. M., Al-Bogami, A. S., Hamza, M. F., & Guibal, E. (2021). 2-Mercaptobenzimidazole-functionalized chitosan for enhanced removal of methylene blue: Batch and column studies. *Journal of Environmental Chemical Engineering*, *9*(4), 0–13. https://doi.org/10.1016/j.jece.2021.105609

Ethaib, S., & Zubaidi, S. L. (2020). Removal of Methylene Blue Dye from Aqueous Solution Using Kaolin. *IOP Conference Series: Materials Science and Engineering*, *928*(2). https://doi.org/10.1088/1757-899X/928/2/022030

Fakher, S., & Imqam, A. (2020). A review of carbon dioxide adsorption to unconventional shale rocks methodology, measurement, and calculation. *SN Applied Sciences*, *2*(1), 1–14. https://doi.org/10.1007/s42452-019-1810-8

Farooq, N., Imran khan, M., Shanableh, A., Mahmood Qureshi, A., Jabeen, S., & ur Rehman, A. (2022). Synthesis and characterization of clay graphene oxide iron oxide (clay/GO/Fe2O3)-nanocomposite for adsorptive removal of methylene blue dye from wastewater. *Inorganic Chemistry Communications*, *145*(August), 109956. https://doi.org/10.1016/j.inoche.2022.109956

Gautam, D., & Hooda, S. (2020). Magnetic Graphene Oxide/Chitin Nanocomposites for Efficient Adsorption of Methylene Blue and Crystal Violet from Aqueous Solutions. *Journal of Chemical and Engineering Data*, *65*(8), 4052–4062. https://doi.org/10.1021/acs.jced.0c00350

Gedam, A. H., Dongre, R. S., & Bansiwal, A. K. (2015). Synthesis and characterization of graphite doped chitosan composite for batch adsorption of lead (II) ions from aqueous solution. *Advanced Materials Letters*, *6*(1), 59–67. https://doi.org/10.5185/amlett.2015.7592

Gemici, B. T., Ozel, H. U., & Ozel, H. B. (2021). Removal of methylene blue onto forest wastes: Adsorption isotherms, kinetics and thermodynamic analysis. *Environmental Technology and Innovation*, *22*, 101501. https://doi.org/10.1016/j.eti.2021.101501

Ghosh, I., Kar, S., Chatterjee, T., Bar, N., & Das, S. K. (2021). Removal of methylene blue from aqueous solution using Lathyrus sativus husk: Adsorption study, MPR and ANN modelling. *Process Safety and Environmental Protection*, *149*, 345–361. https://doi.org/10.1016/j.psep.2020.11.003

Han, S., Yang, J., & Lin, X. (2021). Removal of methylene blue from aqueous solution by functionalized uio-66 with basic moiety. *Desalination and Water Treatment*, *213*, 418–430. https://doi.org/10.5004/dwt.2021.26725

Jaiswal, K. K., Dutta, S., Pohrmen, C. B., Verma, R., Kumar, A., & Ramaswamy, A. P. (2021).

Bio-waste chicken eggshell-derived calcium oxide for photocatalytic application in methylene blue dye degradation under natural sunlight irradiation. *Inorganic and Nano-Metal Chemistry*, *51*(7), 995–1004. https://doi.org/10.1080/24701556.2020.1813769

Jawad, A. H., Saud Abdulhameed, A., Wilson, L. D., Syed-Hassan, S. S. A., ALOthman, Z. A., & Rizwan Khan, M. (2021). High surface area and mesoporous activated carbon from KOH-activated dragon fruit peels for methylene blue dye adsorption: Optimization and mechanism study. *Chinese Journal of Chemical Engineering*, *32*, 281–290. https://doi.org/10.1016/j.cjche.2020.09.070

Ji, L., & Wang, M. (2012). Effect of particle size of natural graphite on methyl blue sorption behavior of expanded graphite. *Advanced Materials Research*, *499*, 12–15. https://doi.org/10.4028/www.scientific.net/AMR.499.12

Kahya, N., & Erim, F. B. (2021). Graphene oxide/chitosan-based composite materials as adsorbents in dye removal. *Chemical Engineering Communications*, *209*(12), 1711–1726. https://doi.org/10.1080/00986445.2021.1986700

Kannan, N., & Sundaram, M. M. (2001). Kinetics and mechanism of removal of methylene blue by adsorption on various carbons - A comparative study. *Dyes and Pigments*, *51*(1), 25–40. https://doi.org/10.1016/S0143-7208(01)00056-0

Ke, C. L., Deng, F. S., Chuang, C. Y., & Lin, C. H. (2021). Antimicrobial actions and applications of Chitosan. *Polymers*, *13*(6). https://doi.org/10.3390/polym13060904

Kim, S. H., Lee, C. M., & Kafle, K. (2013). Characterization of crystalline cellulose in biomass: Basic principles, applications, and limitations of XRD, NMR, IR, Raman, and SFG. *Korean Journal of Chemical Engineering*, *30*(12), 2127–2141. https://doi.org/10.1007/s11814-013-0162-0

Kou, S. (Gabriel), Peters, L. M., & Mucalo, M. R. (2021). Chitosan: A review of sources and preparation methods. In *International Journal of Biological Macromolecules* (Vol. 169). https://doi.org/10.1016/j.ijbiomac.2020.12.005

Kuang, Y., Zhang, X., & Zhou, S. (2020). Adsorption of methylene blue in water onto activated carbon by surfactant modification. *Water (Switzerland)*, *12*(2), 1–19. https://doi.org/10.3390/w12020587

Kyzas, G. Z., Travlou, N. A., Kyzas, G. Z., Lazaridis, N. K., & Deliyanni, E. A. (2015). *Functionalization of Graphite Oxide with Magnetic Chitosan for the Preparation of a Nanocomposite Dye ... Functionalization of Graphite Oxide with Magnetic Chitosan for the Preparation of a Nanocomposite Dye Adsorbent*. *February*. https://doi.org/10.1021/la304696y

Labidi, A., Salaberria, A. M., Fernandes, S. C. M., & Labidi, J. (n.d.). *Functional Chitosan Derivative and Chitin as Decolorization Materials for Methylene Blue and Methyl Orange from Aqueous Solution*. https://doi.org/10.3390/ma12030361

Liu, Q. (2020). Pollution and Treatment of Dye Waste-Water. *IOP Conference Series: Earth and Environmental Science*, *514*(5). https://doi.org/10.1088/1755-1315/514/5/052001

Malatji, N., Makhado, E., Modibane, K. D., Ramohlola, K. E., Maponya, T. C., Monama, G. R., & Hato, M. J. (2021). Removal of methylene blue from wastewater using hydrogel nanocomposites: A review. *Nanomaterials and Nanotechnology*, *11*, 1–27. https://doi.org/10.1177/18479804211039425

Mashkoor, F., & Nasar, A. (2020). Magsorbents: Potential candidates in wastewater treatment technology – A review on the removal of methylene blue dye. *Journal of Magnetism and Magnetic Materials*, *500*(September 2019), 166408. https://doi.org/10.1016/j.jmmm.2020.166408

Mathivanan, M., Syed Abdul Rahman, S., Vedachalam, R., Surya Pavan Kumar, A., SabareeshSabareesh, G., & Karuppiah, S. (2021). Ipomoea carnea: a novel biosorbent for the removal of methylene blue (MB) from aqueous dye solution: kinetic, equilibrium and statistical approach. *International Journal of Phytoremediation*, *23*(9), 982–1000. https://doi.org/10.1080/15226514.2020.1871322

Miraboutalebi, S. M., Nikouzad, S. K., Peydayesh, M., Allahgholi, N., Vafajoo, L., & McKay, G. (2017). Methylene blue adsorption via maize silk powder: Kinetic, equilibrium, thermodynamic studies and residual error analysis. *Process Safety and Environmental Protection*, *106*, 191–202. https://doi.org/10.1016/j.psep.2017.01.010

Moosa, A., Ridha, A., Moosa, A. A., Ridha, A. M., & Kadhim, N. A. (2016). *Use of Biocomposite Adsorbents for the Removal of Methylene Blue Dye from Aqueous Solution*

Use of Biocomposite Adsorbents for the Removal of Methylene Blue Dye from Aqueous Solution. *6*(December), 135–146. https://doi.org/10.5923/j.materials.20160605.03

Murcia-Salvador, A., Pellicer, J. A., Fortea, M. I., Gómez-López, V. M., Rodríguez-López, M. I., Núñez-Delicado, E., & Gabaldón, J. A. (2019). Adsorption of Direct Blue 78 using chitosan and cyclodextrins as adsorbents. *Polymers*, *11*(6). https://doi.org/10.3390/polym11061003

Musa, M. A., & Idrus, S. (2021). Physical and biological treatment technologies of slaughterhouse wastewater: A review. *Sustainability (Switzerland)*, *13*(9), 1–20. https://doi.org/10.3390/su13094656

Myneni, V. R., Kanidarapu, N. R., & Vangalapati, M. (2020). Methylene blue adsorption by magnesium oxide nanoparticles immobilized with chitosan (CS-MgONP): Response surface methodology, isotherm, kinetics and thermodynamic studies. *Iranian Journal of Chemistry and Chemical Engineering*, *39*(6), 29–42. https://doi.org/10.30492/ijcce.2019.36342

Nayl, A. E. A. A., Abd-Elhamid, A. I., Arafa, W. A. A., Ahmed, I. M., El-Shanshory, A. A., Abu-Saied, M. A., Soliman, H. M. A., Abdelgawad, M. A., Ali, H. M., & Bräse, S. (2022). Chitosan-Functionalized-Graphene Oxide (GO@CS) Beads as an Effective Adsorbent to Remove Cationic Dye from Wastewater. *Polymers*, *14*(19). https://doi.org/10.3390/polym14194236

Ngulube, T., Gumbo, J. R., Masindi, V., & Maity, A. (2017). An update on synthetic dyes adsorption onto clay based minerals: A state-of-art review. *Journal of Environmental Management*, *191*, 35–57. https://doi.org/10.1016/j.jenvman.2016.12.031

Oguanobi, N., Collins, O., Chijioke, E., Okechukwu, O., Collins, O. N., & Chijioke Elijah, O. (2019). Adsorption of a Dye (Crystal Violet) on an Acid Modified Non-Conventional Adsorbent. *Journal of Chemical Technology and Metallurgy*, *54*, 95–110.

Oyewo, O. A., Adeniyi, A., Sithole, B. B., & Onyango, M. S. (2020). Sawdust-Based Cellulose Nanocrystals Incorporated with ZnO Nanoparticles as Efficient Adsorption Media in the Removal of Methylene Blue Dye. *ACS Omega*, *5*(30), 18798–18807. https://doi.org/10.1021/acsomega.0c01924

Pashai Gatabi, M., Milani Moghaddam, H., & Ghorbani, M. (2016). Point of zero charge of maghemite decorated multiwalled carbon nanotubes fabricated by chemical precipitation

method. *Journal of Molecular Liquids*, *216*, 117–125. https://doi.org/10.1016/j.molliq.2015.12.087

Pathirana, M. A., Dissanayake, N. S. L., Wanasekara, N. D., Mahltig, B., & Nandasiri, G. K. (2023). Chitosan-Graphene Oxide Dip-Coated Polyacrylonitrile-Ethylenediamine Electrospun Nanofiber Membrane for Removal of the Dye Stuffs Methylene Blue and Congo Red. *Nanomaterials*, *13*(3). https://doi.org/10.3390/nano13030498

Pekakis, P. A., Xekoukoulotakis, N. P., & Mantzavinos, D. (2006). Treatment of textile dyehouse wastewater by TiO2 photocatalysis. *Water Research*, *40*(6), 1276–1286. https://doi.org/10.1016/j.watres.2006.01.019

Quach, T. P. T., & Doan, L. (2023). Surface Modifications of Superparamagnetic Iron Oxide Nanoparticles with Polyvinyl Alcohol, Chitosan, and Graphene Oxide as Methylene Blue Adsorbents. *Coatings*, *13*(8). https://doi.org/10.3390/coatings13081333

Radoor, S., Karayil, J., Jayakumar, A., Parameswaranpillai, J., & Siengchin, S. (2021). Removal of Methylene Blue Dye from Aqueous Solution using PDADMAC Modified ZSM-5 Zeolite as a Novel Adsorbent. In *Journal of Polymers and the Environment* (Vol. 29, Issue 10). https://doi.org/10.1007/s10924-021-02111-8

Rashid, R., Shafiq, I., Akhter, P., Iqbal, M. J., & Hussain, M. (2021). A state-of-the-art review on wastewater treatment techniques: the effectiveness of adsorption method. *Environmental Science and Pollution Research*, *28*(8), 9050–9066. https://doi.org/10.1007/s11356-021-12395-x

Saheed, I. O., Oh, W. Da, & Suah, F. B. M. (2021). Chitosan modifications for adsorption of pollutants – A review. *Journal of Hazardous Materials*, *408*, 124889. https://doi.org/10.1016/j.jhazmat.2020.124889

Santoso, E., Ediati, R., Kusumawati, Y., Bahruji, H., Sulistiono, D. O., & Prasetyoko, D. (2020). Review on recent advances of carbon based adsorbent for methylene blue removal from waste water. *Materials Today Chemistry*, *16*, 100233. https://doi.org/10.1016/j.mtchem.2019.100233

Schirmer, R. H., Adler, H., Pickhardt, M., & Mandelkow, E. (2011). “Lest we forget you - methylene blue...” *Neurobiology of Aging*, *32*(12), 2325.e7-2325.e16.

https://doi.org/10.1016/j.neurobiolaging.2010.12.012

Singh, N., Riyajuddin, S., Ghosh, K., Mehta, S. K., & Dan, A. (2019). Chitosan-Graphene Oxide Hydrogels with Embedded Magnetic Iron Oxide Nanoparticles for Dye Removal. *ACS Applied Nano Materials*, *2*(11), 7379–7392. https://doi.org/10.1021/acsanm.9b01909

Singh, S., Prajapati, A. K., Chakraborty, J. P., & Mondal, M. K. (2023). Adsorption potential of biochar obtained from pyrolysis of raw and torrefied Acacia nilotica towards removal of methylene blue dye from synthetic wastewater. *Biomass Conversion and Biorefinery*, *13*(7), 6083–6104. https://doi.org/10.1007/s13399-021-01645-0

Solayman, H. M., Hossen, M. A., Abd Aziz, A., Yahya, N. Y., Leong, K. H., Sim, L. C., Monir, M. U., & Zoh, K. D. (2023). Performance evaluation of dye wastewater treatment technologies: A review. *Journal of Environmental Chemical Engineering*, *11*(3), 109610. https://doi.org/10.1016/j.jece.2023.109610

Song, X., Zhou, J., Fan, J., Zhang, Q., & Wang, S. (2022). Preparation and adsorption properties of magnetic graphene oxide composites for the removal of methylene blue from water. *Materials Research Express*, *9*(2). https://doi.org/10.1088/2053-1591/ac52c6

Tavakoli, M., Karbasi, S., & Soleymani Eil Bakhtiari, S. (2020). Evaluation of physical, mechanical, and biodegradation of chitosan/graphene oxide composite as bone substitutes. *Polymer-Plastics Technology and Materials*, *59*(4), 430–440. https://doi.org/10.1080/25740881.2019.1653467

Thabede, P. M., Shooto, N. D., & Naidoo, E. B. (2020). Removal of methylene blue dye and lead ions from aqueous solution using activated carbon from black cumin seeds. *South African Journal of Chemical Engineering*, *33*(October 2019), 39–50. https://doi.org/10.1016/j.sajce.2020.04.002

Tichapondwa, S. M., Newman, J. P., & Kubheka, O. (2020). Effect of TiO2 phase on the photocatalytic degradation of methylene blue dye. *Physics and Chemistry of the Earth*, *118–119*, 1–15. https://doi.org/10.1016/j.pce.2020.102900

Tran, T. H., Le, H. H., Pham, T. H., Nguyen, D. T., La, D. D., Chang, S. W., Lee, S. M., Chung, W. J., & Nguyen, D. D. (2021). Comparative study on methylene blue adsorption behavior of coffee husk-derived activated carbon materials prepared using hydrothermal and soaking

methods. *Journal of Environmental Chemical Engineering*, *9*(4), 105362. https://doi.org/10.1016/j.jece.2021.105362

Vasilachi, I. C., Asiminicesei, D. M., Fertu, D. I., & Gavrilescu, M. (2021). Occurrence and fate of emerging pollutants in water environment and options for their removal. *Water (Switzerland)*, *13*(2), 1–34. https://doi.org/10.3390/w13020181

VO, T. S. (2021). Progresses and expansions of chitosan-graphene oxide hybrid networks utilizing as adsorbents and their organic dye removal performances: A short review. *Journal of the Turkish Chemical Society Section A: Chemistry*, *8*(4), 1121–1136. https://doi.org/10.18596/jotcsa.943623

Wang, W., Xue, C., & Mao, X. (2020). Chitosan: Structural modification, biological activity and application. *International Journal of Biological Macromolecules*, *164*, 4532–4546. https://doi.org/10.1016/j.ijbiomac.2020.09.042

Yan, M., Huang, W., & Li, Z. (2019). Chitosan cross-linked graphene oxide/lignosulfonate composite aerogel for enhanced adsorption of methylene blue in water. *International Journal of Biological Macromolecules*, *136*, 927–935. https://doi.org/10.1016/j.ijbiomac.2019.06.144

Yunusa, U., Usman, B., & Bashir Ibrahim, M. (2021). Algerian Journal of Chemical Engineering Cationic dyes removal from wastewater by adsorptive method: A systematic in-depth review. *Algerian Journal of Chemical Engineering*, *02*, 6–40. http://www.journal.acse.science/index.php/ajce/indexhttp://dx.doi.org/10.5281/zenodo.5101197

Zango, Z. U., Dennis, J. O., Aljameel, A. I., Usman, F., Ali, M. K. M., Abdulkadir, B. A., Algessair, S., Aldaghri, O. A., & Ibnaouf, K. H. (2022). Effective Removal of Methylene Blue from Simulated Wastewater Using ZnO-Chitosan Nanocomposites: Optimization, Kinetics, and Isotherm Studies. *Molecules*, *27*(15). https://doi.org/10.3390/molecules27154746

Zhang, W., Zhou, C., Zhou, W., Lei, A., Zhang, Q., Wan, Q., & Zou, B. (2011). Fast and considerable adsorption of methylene blue dye onto graphene oxide. *Bulletin of Environmental Contamination and Toxicology*, *87*(1), 86–90.

https://doi.org/10.1007/s00128-011-0304-1

Zhou, Y., Lu, J., Zhou, Y., & Liu, Y. (2019). Recent advances for dyes removal using novel adsorbents: A review. *Environmental Pollution*, *252*, 352–365. https://doi.org/10.1016/j.envpol.2019.05.072

Zhu, W., Jiang, X., Liu, F., You, F., & Yao, C. (2020). Preparation of chitosan-graphene oxide composite aerogel by hydrothermal method and its adsorption property of methyl orange. *Polymers*, *12*(9). https://doi.org/10.3390/POLYM12092169

Appendix

Appendix A: The Effect of Chitosan/graphite Mixing Ratio, and Particle Size on the Removal

Table A-1: Effect of chitosan/graphite mixing ratio on the removal of methylene blue dye using chitosan/graphite composite synthesized with (1:3, 1:1 and 3:1) ratios

Chitosan/graphite mixing ratio	Particle size (nm)	Experiments (absorbance)			Absorbance Mean ± Std.)	Removal efficiency (%)
		1	2	3		
25:75	250-500	1.42	1.4	1.38	1.4±0.013	25.98
50:50	250-500	1.1	1.2	1.38	1.1±0.126	42.05
75:25	250-500	0.72	0.74	0.73	0.730±0.006	67.87

Table A-2: Effect of particle size on the removal of methylene blue dye using chitosan/graphite composite

Particle size (µm)	Experiments (absorbance)			Absorbance (Mean ±Std.)	Removal efficiency (%)
	1	2	3		
125-150	0.730	0.731	0.732	0.731±0.01	61.82
150-250	1.05	1.07	1.00	1.041±0.032	45.23
250=300	1.281	1.283	1.282	1.283±0.02	38.5

Appendix B:-Point of Zero Charge Analysis for Chitosan/Graphite Composite

Table B-1: Point of zero charge for chitosan/graphite composite

Initial pH	Final pH	ΔpH (Pf-Pi)
2.04	3.28	1.24
3.02	5.36	2.34
4.02	7.46	3.44
4.98	5.65	0.67
6.05	5.67	-0.38
7.02	5.62	-1.4
7.98	5.75	-2.23
9.01	5.84	-3.17
10	6.07	-3.93
11	6.06	-4.94

Appendix C: Individual Effect of Operating Parameters on Removal of Methylene Blue Dye

Table C-1: Effect of pH of the solution on the removal of methylene blue dye using chitosan/graphite composite

	Experiments (absorbance)			Absorbance	
Initial concentration	1	2	3	(Mean ±Std.)	Removal efficiency (%)
2	1.455	1.454	1.453	1.453±0.01	23.15
4	1.390	1.398	1.99	1.396±0.37	25.2
6	1.19	1.191	1.193	1.191±0.01	37.18
8	0.81	0.812	0.813	0.812±0.01	57.48
10	0.479	0.478	0.491	0.479±0.0067	77.12
12	0.45	0.5	0.48	0.477±0.023	77.19

Table C-2: Effect of initial concentration of methylene blue dye

Initial concentration (mg/L)	Experiments (absorbance)			Absorbance (Mean ±Std.)	Removal efficiency (%)
	1	2	3		
5	0.186	0.187	0.188	0.187±0.01	81.91%
10	0.45	0.42	0.46	0.44±0.017	77.4%
15	1.28	1.31	1.32	1.3±0.33	54.22%
20	2.4	2.3	2.2	2.3±0.1	38.89%

Table C-3: Effect of contact time

Contact time (min)	Experiments (Absorbance)			Absorbance	Removal efficiency (%)
	1	2	3	(Mean ± Std.)	
30	1.21	1.175	1.18	1.188±0.004	21.18
60	0.523	0.53	0.518	0.52±0.11	73.7
90	0.356	0.350	0.352	0.354±0.0012	82
120	0.281	0.278	0.29	0.28±0.005	85.98
150	0.262	0.263	0.267	0.265±0.019	86.8

Appendix D: Adsorption Isotherm and Kinetic Model Data

Table D-1: Equilibrium data for adsorption isotherm model

Ci(mg/L)	Experiments absorbance)			Mean ±Std.					
	1	2	3		Ce	Qe	Ce/Qe	ln(Ce)	ln(Qe)
5	0.037	0.0369	0.0368	0.03687±0.0027	0.1	2.45	0.04	-2.3	0.896
10	0.29	0.3	0.292	0.29825±0.007	1.5	4.25	0.3529	0.405	1.4469
15	0.657	0.69	0.68	0.679±0.0016	3.54	5.73	0.617	1.264	1.74
20	1.1	1.05	1.04	1.063±0.01	5.6	7.2	0.778	1.73	1.97

Table D-2: Equilibrium data for adsorption kinetics models

Time (min)	Ci (mg/L)	Experiments (Absorbance)			Absorbance (mean +Std.)	Ct(mg/L)	Qe (mg/L)	Qt (mg/L)	Ln (Qe-Qt)	t/Qt
		1	2	3						
20	5	0.825	0.817	0.818	0.82±0.06	4.1	0.45	2.45	2	44.44
40	5	0.789	0.785	0.786	0.787±0.016	3.76	0.62	2.45	1.83	64.52
60	5	0.76	0.759	0.78	0.77±0.01	3.6	0.7	2.45	1.75	85.71
80	5	0.753	0.754	0.750	0.752±0.04	3.4	0.8	2.45	1.65	100
100	5	0.749	0.762	0.753	0.75+0.036	3.38	0.81	2.45	1.64	123.46

Appendix E: Data from Design Expert Model Fitting

Table E-1: Model summary of statistics for methylene blue dye removal

Source	Std. Dev.	R^2	Adjusted R^2	Predicted R^2	PRESS	
Linear	8.63	0.7478	0.6897	0.5891	1576.39	
2FI	8.65	0.8049	0.6879	0.4837	1980.50	
Quadratic	**0.9276**	**0.9984**	**0.9964**	**0.9931**	**26.44**	**Suggested**
Cubic	1.10	0.9987	0.9949		*	Aliased

Table E-2: Fit statics for methylene blue dye removal

Std. Dev.	0.9276	**R^2**	0.9984
Mean	66.05	**Adjusted R^2**	0.9964
C.V. %	1.40	**Predicted R^2**	0.9931
		Adeq Precision	67.6127

Figure 4. 17: Some experimental photos